Investigations of Photosystem-II-Mutants in the diatom *Phaeodactylum tricornutum*

Diplomarbeit

von Sabine Ng Chin Yue

im Oktober 2005

angefertigt am Lehrstuhl für Pflanzliche Ökophysiologie
Universität Konstanz

Zusammenfassung

In dieser Arbeit wurden vier verschiedene Mutanten der Kieselalge *Phaeodactylum tricornutum* charakterisiert. Alle Mutationen liegen im D1 Protein des Photosystems II (PS II) und befinden sich innerhalb bzw. in näherer Umgebung der Q_B-Bindetasche. Ein Aminosäurenaustausch von Valin zu Isoleucin in Position 219 (VI-219), Phenylalanin zu Isoleucin in Position 255 (FI-255), Serin zu Alanin in Position 264 (SA-264) und Leucin zu Tryptophan in Position 275 (LW-275) wurden festgestellt. Neben der genetischen Charakterisierung wurden verschiedene physiologische Messungen durchgeführt, um den Einfluss der Mutationen auf die Photosynthese zu untersuchen. Untersuchungen zur Elektronentransport-Rate und Resistenz gegen DCMU als auch Messungen zur Struktur des photosynthetischen Apparates wurden gemacht. Des Weiteren wurden zwei verschiedene Lichtschutz-Mechanismen untersucht, die die Zellen vor Licht schützen sollen. Diese sind das so genannte non-photochemical fluorescence quenching (NPQ), ein Prozess bei dem überschüssige Energie in Wärme umgewandelt wird sowie der Elektronenzyklus um das PS II. In VI-219 wurde nur eine schwache Minderung des Elektronentransportes von Q_A nach Q_B im Vergleich zum Wild-Typ (WT) gemessen und auch die Resistenz gegen DCMU war niedrig (Faktor 3). Die Menge an PS II und die Antennengröße pro PS II Reaktionszentrum unterschieden sich nur geringfügig von den Werten, die für den WT gefunden wurden. Dies galt auch für die NPQ-Werte und den PS II Zyklus. In FI-255 dagegen war die Elektronentransport-Rate um den Faktor 2.7 vermindert. Eine 300-fache Resistenz gegen DCMU wurde festgestellt, sowie eine Zunahme an PS II und eine gleichzeitige Verkleinerung der Antennengröße pro PS II. Die Werte für NPQ waren niedriger als im WT, was einen verminderten Lichtschutz bedeutet. Ein Maximum von etwa 6 Elektronen kreisen hier um das Photosystem II, was dem 1,5 fachen des maximalen PS II Zyklus im WT (4 Elektronen) entspricht. SA-264 war um den gleichen Faktor wie FI-255 im Elektronentransport inhibiert, zeigte aber eine sehr hohe Resistenz gegen DCMU (3000-fach). Wie in FI-255 wurde auch hier eine Zunahme der PS II Reaktionszentren und damit des D1 gemessen sowie eine Verkleinerung der Antennengröße. Die Werte für NPQ sowie für den PS II Zyklus waren sehr gering. In LW-275 konnte die höchste Inhibierung des Elektronentransfers von Q_A nach Q_B gemessen werden mit einem Faktor von 1.5.

Das bedeutet, dass während im WT 3 Elektronen transportiert werden, können in der LW-275 Mutante in derselben Zeit nur 2 Elektronen weitergereicht werden. Neben der Resistenz gegen DCMU konnte auch hier wie in den Mutanten FI-255 und SA-264 eine Zunahme des PS II und eine Verringerung der Antennengröße beobachtet werden. Ausserdem wurde hier auch die Anzahl an PS I pro PS II erhöht. LW-275 besitzt die niedrigsten Werte für NPQ und hat mit 7 Elektronen die höchste Anzahl an Elektronen, die um das PS II kreisen was auf hohe Lichtempfindlichkeit schließen lässt. Dies konnte in Starklicht Experimenten bestätigt werden.

Neben den physiologischen Messungen wurden Vorbereitungen für Gen-Expressionsanalysen durchgeführt. Da die Expression verschiedener Proteine des Chloroplasten, die im Zellkern kodiert sind, vom Redoxzustand des Plastochinon-Pools abhängt, sollten Expressionsanalysen vorbereitet werden. In dieser Arbeit wurden erfolgreich Hybridisierungssonden hergestellt, quantifiziert und getestet.

Die hier vorgestellten Mutanten sind die ersten photosynthetischen Mutanten in einer Kieselalge. Durch die Charakterisierung konnten Erkenntnisse über die Bedeutung der vier Aminosäuren im Elektronentransport und im Lichtschutz gewonnen werden. Dabei zeigte sich insbesondere, dass, abgesehen von den Aminosäuren innerhalb bzw. in unmittelbarer Nähe der Q_B Bindetasche (Pos. 255 und 264), die Aminosäure an der Position 275 eine entscheidende Rolle in der Funktionalität des Photosystems II zu spielen scheint.

Table of Contents

Abbreviations

AA	amino acid
ADP	adenosine diphosphate
Amp	ampicillin
APS	ammonium persulfate
ATP	adenosine triphosphate
a.u.	arbitrary units
BCIP	5-bromo-4-chloro-3-indolyl phosphate
bp	base pairs
c	concentration
°C	degree Celsius
cDNA	copy desoxyribonucleic acid
Chl	chlorophyll
Chl*	excited chlorophyll
cm	centimetre (s)
CO_2	carbon dioxide
Cyt	cytochrome
DCMU	3-(3,4-dichlorophenyl)-1,1-dimethylurea
DD	diadinoxanthin
DDE	diadinoxanthin de-epoxidase
DEPC	di-ethyl pyrocarbonate
DF	dilution factor
DIG	digoxigenin
DMSO	dimethyl sulfoxide
DNA	desoxyribonucleic acid
DT	diatoxanthin
DTT	dithiothreitol
e^-	electron (s)
ECL	enhanced chemiluminescence
E.coli	*Escherichia coli*
EDTA	ethylenediamintetraacetic acid
e.g.	example given
EtBr	ethidium bromide

EtOH	ethanol
F_0	minimal level of chlorophyll fluorescence
F_m	maximal level of chlorophyll fluorescence
F_v	variable fluorescence
Fd	ferredoxin
Fig.	figure
FNR	ferredoxin-$NADP^+$ reductase
g	gravity acceleration
g/L	gram (s) per litre
h	hour (s)
H^+	proton (s)
HL	high light
IPTG	isopropyl β-D-thiogalactopyranoside
J	Joule (s)
kb	kilo basepairs
kDa	kilo Dalton
L	litre (s)
*lac*Z	gene of the N-terminal α-fragment of β-galactosidase
LB	Luria-Bertani
LED	light emitting diode
LHC	light harvesting complex
LL	low light
m	metre (s)
M	molar
mA	milliampere (s)
MF	multiplication factor
mg	milligram (s)
min	minute (s)
mL	millilitre (s)
mM	millimolar
Mn	manganese
MOPS	3-[N-morpholino]-propane sulphuric acid
NADP	nicotinamid adenine dinucleotide phosphate
NBT	nitrobluetetrazolium

ng	nanogram (s)
nm	nanometer (s)
NPQ	non-photochemical quenching
O_2	oxygen
OD	optical density
OD_i	optical density at a wavelength of (i) nm
OEC	Oxygen Evolving Complex
oligo d(T)	oligo-deoxythymidine
PAGE	polyacrylamide gel electrophoresis
PAM	pulse amplitude modulated fluorometer
PBS	phosphate buffered saline
PC	plastocyanine
PCR	polymerase chain reaction
PM	photo multiplier
PMSF	phenylmethylsofonyl fluoride
PQ	plastoquinone
PQH	plastoquinol
PS I	photosystem I
PS II	photosystem II
*psb*A	gene of the D1 protein
PTFE	polytetrafluoroethylene
PVDF	polyvinylidenedifluoride
Q_A	primary plastoquinone electron acceptor of PS II
Q_B	secondary plastoquinone electron acceptor of PS II
RC	reaction centre
RNA	ribonucleic acid
RNase	ribonuclease
rpm	rounds per minute
s	second (s)
S_o-S_4	different oxidation states of the oxygen evolving complex
SDS	sodium dodecyl sulfate
SSC	saline sodium citrate
TAE	tris-acetate-EDTA buffer
Taq	*Thermus aquaticus*

TB	transformation buffer
TEMED	N, N, N´, N´ tetra methyl-ethylene diamine
Tris	Tris(hydroxymethyl)-aminomethane
u	unit (s)
UV	ultraviolet radiation
V	volt (s)
(v/v)	volume per volume
(w/v)	weight per volume
x	times (e.g. 30x: 30 times)
X-Gal	5-Bromo-4-Chloro-3-Indolyl-β-D-Galactopyranoside
Y_{SS}	steady state yield
Y_Z	tyrosine Z of the PS II reaction centre
ΔpH	transthylakoidal proton gradient
µg	microgram (s)
µL	microlitre (s)
µm	micrometer (s)
µmol	micromole (s)
%	percent

1 Introduction

1.1 Oxygenic Photosynthesis

1.1.1 General Function of the photosynthetic System: Photochemistry

The reactions of photosynthesis can be divided into two steps. The first step takes place in the thylakoid membranes of the chloroplasts where the photochemical reactions and the transfer of electrons are found. Light energy is converted into chemical energy in the form of ATP and NADPH, while simultaneously water is oxidized and oxygen (O_2) is released. A transfer of protons is coupled to the electron transport. The second step which is found in the stroma of the plastids, is the assimilation (reduction) of CO_2 in the Calvin cycle. During this reaction, part of the previously produced NADPH and ATP molecules are used.

Four complexes are responsible for the charge separation, electron transfer and production of NADPH and ATP. In figure 1.1 those four complexes which are found in the thylakoid membrane and allow oxygenic photosynthesis are shown: the photosystem II (PS II), the cytochrome (cyt) b_6/f complex, photosystem I (PS I) and the ATP synthase which uses the transthylakoidal proton gradient to synthesize ATP from ADP.

Each photosystem consists of two parts: the reaction centre (RC) and the antenna complex which is transmitting the excitation energy from the light to the reaction centre. The PS II reaction centre is composed of the two proteins D1 and D2, which carry all cofactors necessary for the initial charge separation, cytochrome b-559 as well as several other polypeptides. The accessory pigments and Chl *a* catch the light energy and transfer it from pigment to pigment until it reaches the reaction centre. In the centre of the PS II, P680, charge separation takes place: the energy is used to excite the chlorophyll centre, thereby forming P680* (reductant) which rapidly transfers an electron to an adjacent pheophytin (chlorophyll without magnesium) and becomes $P680^+$. Thanks to the electrons resulting from the oxidation of water ($2H_2O \rightarrow O_2 + 4H^+ + 4e^-$), the excited chlorophyll $P680^+$ is able to return very rapidly

to its stable state P680. The oxidation of water takes place at the manganese cluster of the oxygen evolving complex, which is located at the PS II.

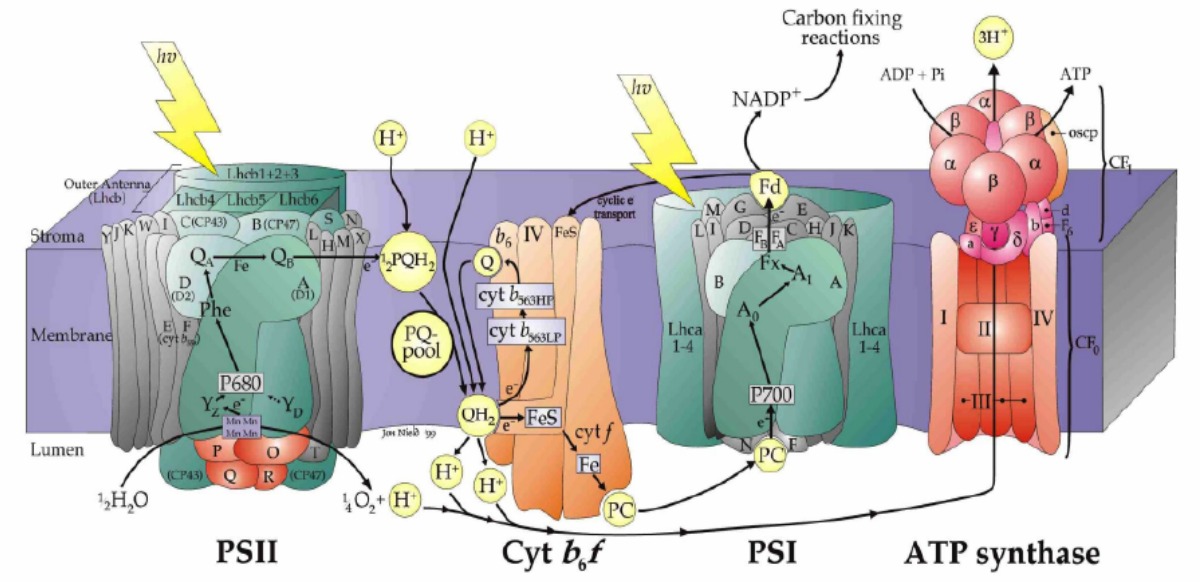

***Fig. 1.1*: Scheme of the Electron Transport Chain in the Eukaryotic Thylakoid Membrane.** PS I and PS II: photosystem I and II, Cyt: cytochrome, PQ: plastoquinone, PC: plastocyanine, Fd: ferredoxin. (figure from Nield, 1999)

Pheophytin is the initial acceptor which receives an electron from the P680* and transfers it to the primary and secondary acceptors which are two plastoquinone molecules (Q_A and Q_B). Q_A is located at the centre while Q_B is mobile. Q_B is part of the plastoquinone (PQ) pool which is found in the membrane of the thylakoids. It is reduced twice (after two charge separations) and protonated by two H^+ coming from the stroma. This Q_BH_2 form (plastoquinol) is mobile and contributes to the PQH_2 pool in the membrane while another oxidized PQ molecule refills the Q_B binding niche at the D1 protein. The electrons are then transferred from the reduced plastoquinones (PQH_2) to the cyt *b_6/f* complex and subsequently to plastocyanine, a hydrophilic soluble protein which is mobile in the lumen. Plastocyanine transfers the electrons to the Chl-centre of the PS I, P700. After light-driven charge separation, the electrons are transferred via several steps from P700 to a soluble ferredoxin at the stroma side of the thylakoid membrane. The final electron acceptor $NADP^+$ is reduced by ferredoxin via the activity of a flavoprotein, the ferredoxin-$NADP^+$ reductase (FNR). The NADPH is then used for reduction processes by the enzymes of the Calvin cycle. The energy of the photons is not only used for the production of NADPH molecules, but also for the synthesis of ATP molecules. The transfer of electrons is coupled with the translocations of protons. At PS II for each liberated O_2 four protons are

transferred in the lumen. Additionally, the double reduction of Q_B which is accompanied by its protonation of two protons from the stroma contributes to the proton-pool in the lumen, when PQH_2 is oxidized and the protons are liberated in the lumen. A transthylakoidal proton gradient (ΔpH), the proton motor force is used by the ATP-synthase to phosphorylate ADP on the stroma side and therefore producing ATP.

In the following chapters, the emission of two inevitable 'by-products' of the photochemical process, oxygen and chlorophyll fluorescence, are described. Those two factors were used during this work to assess the photosynthetic activity and its regulation.

1.1.2 Oxygen Evolution at the Oxygen Evolving Complex (OEC)

As described by Diner and Babcock (1996) light-induced charge separation in PS II occurs at the P680 chlorophyll moiety, which is bound at the interface of the D1/D2 heterodimer that forms the protein core of PS II. The $P680^+$ chlorophyll cation is formed by the transfer of electrons which are provided from the oxidation of water ($2H_2O \rightarrow O_2 + 4H^+ + 4e^-$) is a strong oxidant which rapidly oxidizes a nearby tyrosine designated Y_Z. This redox active tyrosine is conventionally thought of as the lone electron transfer intermediate between $P680^+$ and the oxygen evolving complex (OEC). The core of the OEC is a cluster of four manganese (Mn) ions. After four oxidation equivalents are transferred from the OEC, molecular oxygen is liberated, and the OEC reaches again its most reduced state.

Details of the oxygen evolving cycle were described by Kok (1970), and the cycle involving five so-called S-state intermediates is also termed the Kok cycle or the S-state cycle (Fig. 1.2). S-state transitions represent single electron oxidations of the OEC, caused by electron transfer through Y_Z to rereduce $P680^+$. The most reduced state, S_0, is formed after molecular oxygen is released from a previous cycle. Photon absorption and electron transfer from P680 lead to the formation of the highly oxidizing $P680^+$ cation, which oxidizes Y_Z to Y_Z*. In turn, Y_Z* extracts an electron from the OEC inducing the $S_0 \rightarrow S_1$ transition. Subsequent photon absorption by P680 drive the $S_1 \rightarrow S_2$, $S_2 \rightarrow S_3$, and $S_3 \rightarrow S_4$ transitions. S_4 is an unstable activated complex which releases molecular oxygen on the timescale of 1 ms, resetting the cycle.

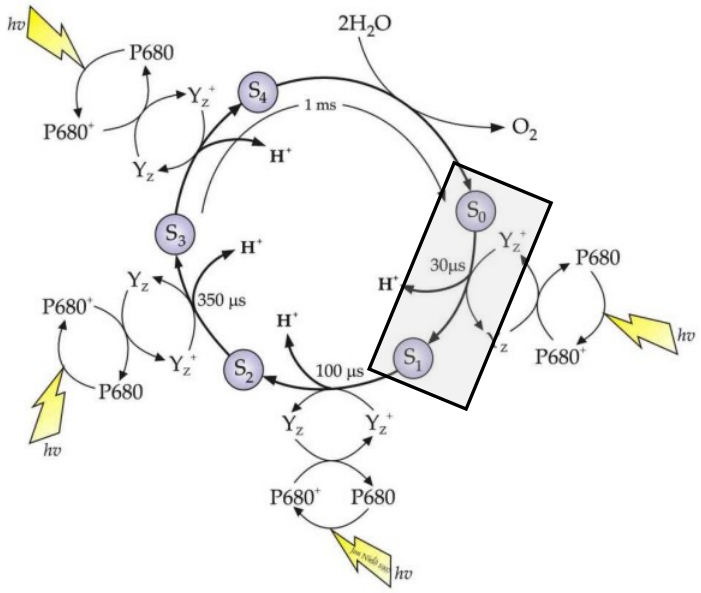

***Fig 1.2*: The S-state Cycle for the Oxygen evolving Reactions of PS II** (Kok *et al.*, 1970). Dark-stable states are boxed. In the dark 25 % - 35 % are in state S_0 and 65 % - 75 % are in state S_1. Diagram adapted from Rutherford (1989).

1.1.3 Chlorophyll Fluorescence Emission

When light is absorbed by the antenna pigments, it is subsequently transferred to the chlorophyll centre, where it excites the Chl *a* centre molecule. There are three ways for the excited Chl* to be inactivated (fig. 1.3):

1. Photochemistry: the energy is transferred to the Chl-centre. Charge separation takes place, the excited Chl* is oxidized loosing one electron to a primary acceptor, from where the electron is transported through the photosynthetic electron transport chain (see 1.1). More than 90 % of the excited chlorophyll molecules are inactivated this way.
2. Fluorescence: the energy is re-emitted as photons of fluorescence.
3. Heat dissipation: the energy is re-emitted as heat.

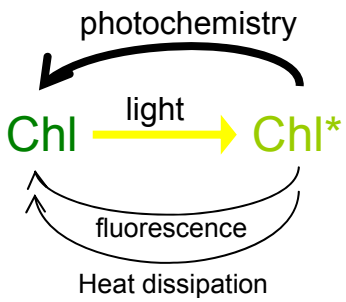

***Fig. 1.3*: The three Ways to inactivate the excited Chlorophyll (Chl*).**

In recent years, the technique of measuring chlorophyll fluorescence has become ubiquitous in plant ecophysiology studies. The principle underlying chlorophyll fluorescence analysis is relatively straightforward. As described before, light energy absorbed by chlorophyll molecules can undergo one of three fates: it can be used to drive photosynthesis (photochemistry), excess energy can be dissipated as heat or it can be re-emitted as light (chlorophyll fluorescence). These three processes are competing; any increase in the efficiency of one process will result in a decrease in the yield of the other two processes. Hence, by measuring the yield of chlorophyll fluorescence, information about changes in the efficiency of photochemistry and heat dissipation can be obtained.

Although chlorophyll fluorescence is usually very weak (only 1 or 2 % of total light absorbed), measurement of fluorescence is quite easy. The spectrum of fluorescence is different to that of absorbed light, with the peak of fluorescence emission being of longer wavelength than that of absorption. Therefore, fluorescence yield can be quantified by exposing a leaf to light of defined wavelength and measuring the amount of light re-emitted at longer wavelengths.

Changes in the yield of chlorophyll fluorescence were first observed by Kautsky (Kautsky *et al.*, 1960). He found that, upon transferring photosynthetic material from the dark into the light, an increase in the yield of chlorophyll fluorescence occurred over a time period of around 1 s. This rise has subsequently been explained as a consequence of reduction of electron acceptors in the photosynthetic pathway, downstream of PS II, notably quinone and in particular Q_A. Once PS II absorbs light and Q_A has accepted an electron, it is not able to accept another electron until it has passed the first one onto a subsequent electron carrier (Q_B). During this period, the reaction centre is said to be ‘closed’. At any time, the presence of a proportion of closed reaction centres leads to an overall reduction in the efficiency of photochemistry and so to a corresponding increase in the yield of fluorescence.

When a leaf is transferred from darkness into light, PS II reaction centres are progressively closed. This gives rise (during the first milliseconds to seconds of illumination) to an increase in the yield of chlorophyll fluorescence. Subsequently the fluorescence level typically starts to fall again over a period of a few minutes. This phenomenon, termed fluorescence quenching, is explained in two ways. First, there is an increase in the rate of electron transport from PS II; this is mainly due to the light-induced activation of enzymes involved in carbon metabolism. Such quenching

is referred to as ‘photochemical quenching’. At the same time there is an increase in the efficiency with which energy is converted to heat. This latter process is termed ‘non-photochemical quenching’ (NPQ). This process avoids an over-reduction of the PSII when the cells are exposed to a light intensity which exceeds the capacity for photochemistry. It thereby provides the photosynthetic apparatus with an efficient way to protect (so-called photoprotection) from the oxidative damages (generated by an accumulation of unused energy) which leads to damage of the photosynthetic apparatus and consequently a decrease in the photosynthetic potential (so-called photoinhibition).

In order to gain useful information about the photosynthetic performance of a plant from measurements of the chlorophyll fluorescence yield, it is necessary to be able to distinguish between the photochemical and non-photochemical contributions to quenching. The usual approach is to ‘switch off’ one of the two contributors, specifically photochemistry, so that the fluorescence yield in the presence of the other alone can be estimated. *In vitro* this can be achieved by the addition of chemicals, such as the herbicide DCMU that inhibits PS II and therefore reduces photochemistry to zero. This method, however, is both impractical and undesirable in a more physiological context. Instead, a new method has been developed, the ‘light doubling’ technique (Quick and Horton, 1984). In this system, the light source used to measure fluorescence is switched on and off very rapidly and the detector is tuned to detect only fluorescence excited by the measuring light. Therefore, the relative yield of fluorescence can now be measured in the presence of background illumination.

During this study two different instruments were used to measure chlorophyll fluorescence, a conventional fluorometer and a pulse amplitude modified (PAM) fluorometer. Details of the instruments and the fluorescence levels measured with these apparatus are described in 2.5.2.

1.2 The Diatoms

1.2.1 General description

Diatoms are a group of unicellular algae that colonize the oceans and freshwater habitats. They are thought to be the most important group of eukaryotic phytoplankton, responsible for approximately 40 % of marine primary productivity

(Falkowski *et al*., 1998). They belong to the class Bacillariophyceae within the division of Heterokontophyta. Their most characteristic feature is the ability to generate a highly patterned external wall composed of amorphous silica [$(SiO_2)n(H_2O)$], known as frustule. This is often constructed of two almost equal halves, with the smaller fitting into the larger like a Petri dish. The larger of the two halves is denoted the epitheca, and the inner one is denoted the hypotheca (Fig. 1.4).

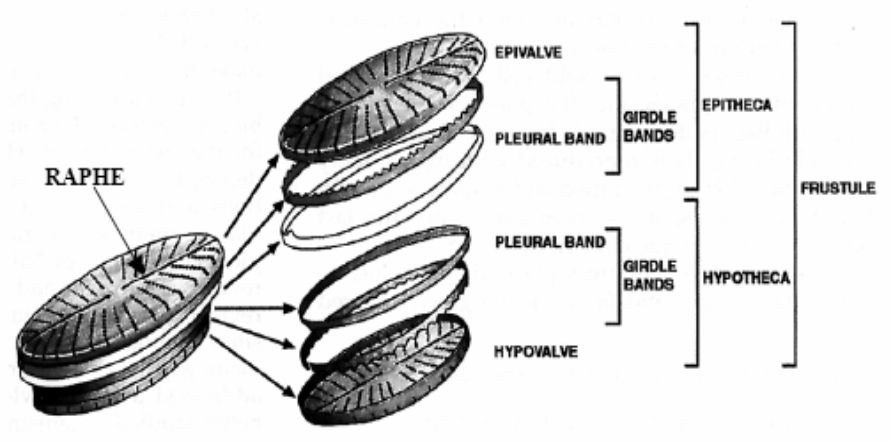

***Fig. 1.4*: Schematic Overview of the Components of the Frustule of a pennate Diatom.** (modified after Zurzolo and Bowler, 2001)

Diatoms are generally classified into two major groups depending on the symmetry of their frustules (Kooistra *et al*., 2003). Centric diatoms are radially symmetrical, whereas pennate diatoms are elongated and bilaterally symmetrical. The former group tends to be planktonic, while the latter are benthic, living on sediments or other surfaces like stones.

Like in other photosynthetic eukaryotes, the photosynthetic apparatus of diatoms is housed within plastids inside the cell. The thylakoid membrane within the plastid have the typical structure of the Heterokontophyta, grouped into stacks (lamellae) of three, all enclosed by a girdle lamella (van den Hoek *et al*., 1997). Diatoms are brown in colour owing to the presence of the accessory carotenoid pigment fucoxanthin, which is located together with chlorophyll *a* and *c* in their plastids. Fucoxanthin and chlorophylls are bound within the light-harvesting antenna complexes by fucoxanthin, chlorophyll *a*/*c*-binding proteins (FCP) (Owens, 1986).

1.2.2 Evolution of the Diatoms

The plastids of all photosynthetic organisms are likely to have arisen at least 1.5 billion years ago form the engulfment of a photosynthetic bacterium by a unicellular eukaryotic heterotroph (van den Hoek *et al*., 1997). Current knowledge suggests that the initial endosymbiotic event gave rise eventually to two major plastid lineages: chloroplasts and rhodoplasts. Green algae, as well as their descendants, the higher plants, contain chloroplasts that are characterized by the presence of stacked thylakoid membranes and the use of chlorophyll *a* and *b* for light harvesting. Red algae, on the other hand, contain rhodoplasts, which use chlorophyll *a* and phycobilisomes to capture light energy (Fig. 1.5).

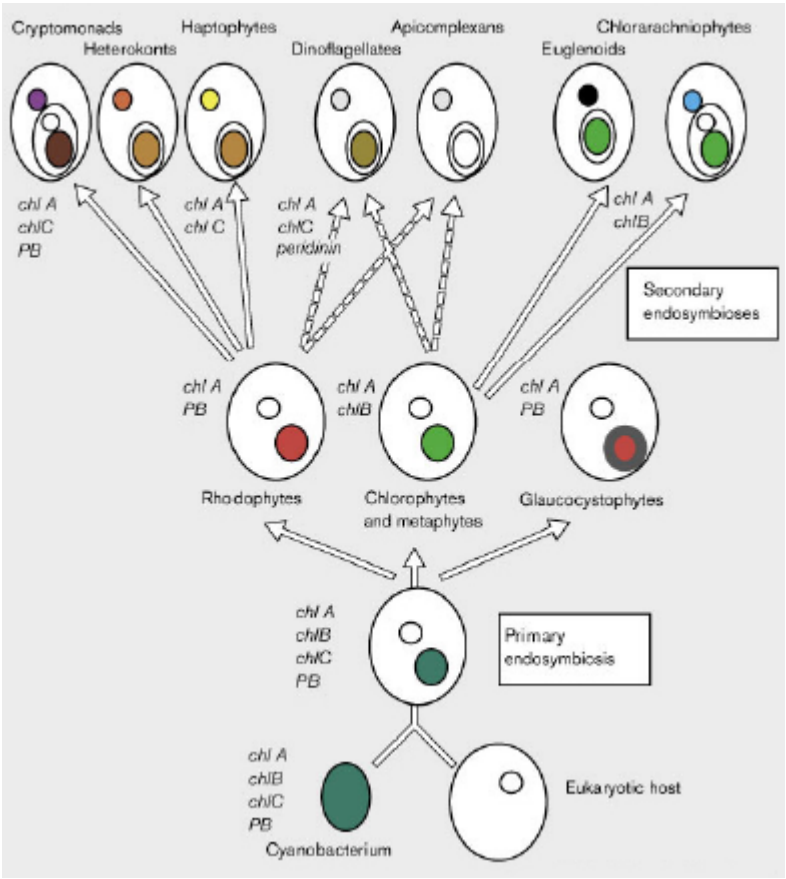

***Fig. 1.5*: Hypothetic Scheme of the Origin of Plastids of photosynthetic Organisms.** Figure is based on the theory of primary and secondary endosymbiosis. Cell nuclei are represented by a white circle while plastids are represented as coloured circles. Each circle surrounding the plastids is equivalent with two membranes (Douglas, 1998).

Chromophyte algae, such as diatoms, differ fundamentally from the majority of photosynthetic eukaryotes: whereas the plastids of red algae, green algae and plants

are normally surrounded by two membranes, diatom plastids have four membranes. It is therefore believed that diatoms and related chromophyte algae arose following a secondary endosymbiotic event in which a eukaryotic alga was engulfed by a second eukaryotic heterotroph (Delwiche and Palmer, 1997). The endosymbiont originally possessed a nucleus, chloroplasts as well as mitochondria and other organelles (Fig. 1.6). After establishment of secondary endocytobiosis all these organelles vanished with the exception of the plastids.

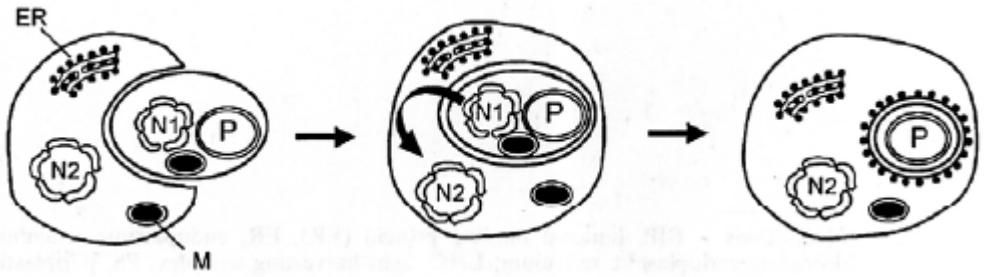

***Fig. 1.6*: Putative Evolution of Diatom Plastids.** After engulfing a photosynthetic eukaryotic red alga by a eukaryotic host cell, a massive gene transfer from the nucleus of the endosymbiont (N1) to the nucleus of the host cell (N2) must have occurred (bent arrow). Degradation of nucleus, mitochondria (M) and other cytosolic structures of the endosymbiont results in plastids (P) with four bounding membranes, with the outermost membrane being transformed into an ER (endoplasmic reticulum) -type membrane (Kroth and Strotmann, 1999).

It seems obvious that the inner two membranes of the chromophyte plastids represent the two envelope membranes of the plastid of the eukaryotic endosymbiont. However, the origin of the two outer membranes is still unclear. According to the theory of secondary endocytobiosis, the outer membranes may descend from the plasma membrane of the endosymbiont plus the phagotrophic membrane of the host cell (Whatley *et al*., 1979).

1.2.3 Diatoms and Light

Diatoms experience large fluctuations in light intensity due to unpredictable water motions that can vary over several orders of magnitude (Falkowski and Raven, 1997). In order to minimize photoinhibition (PS II damage caused by light) that could result from periodic exposure to excess light energy when the cell are transported to the water column surface, they have developed efficient photoprotective mechanisms (Ting and Owens, 1993; Lavaud *et al.*, 2002b and 2002c). The nonradiative dissipation of the light energy absorbed in excess is an important mechanism (Niyogi,

2000). This phenomenon is attributed to rapid modifications within the light-harvesting complexes (LHC) of PS II leading to a decrease in the excitation pressure on PS II. It is designated nonphotochemical fluorescence quenching (NPQ) and can be measured as a decrease in chlorophyll fluorescence intensity under high light (see 1.1.3). In higher plants and green algae, NPQ is controlled by the formation of a proton gradient (ΔpH) across the thylakoid membrane and by reversible conversion of epoxidized (violaxanthin) and de-epoxidized (antheraxanthin and zeaxanthin) forms of xanthophylls (the so-called xanthophyll cycle; for reviews see Müller *et al*., 2001). The xanthophyll cycle in diatoms consists of the conversion of the monoepoxide diadinoxanthin (DD) into the de-epoxide diatoxanthin (DT) under excess light and vice versa under limiting light or darkness (Hager and Stransky, 1970). In diatoms, NPQ depends on the size of the DD pool and can reach much larger values than in higher plants (Lavaud *et al*., 2002c). Failure of this protection leads photoinhibition (Lavaud *et al*., 2002c).

It was shown that photo-oxidative damage is also prevented by an electron transfer cycle around PS II (Lavaud *et al*., 2002b). Cyclic electron flow around PS II has been suggested earlier as a photoprotection mechanism that could retard both acceptor and donor side photoinhibition (Nebdal *et al*., 1992). If electrons are provided by a cyclic electron transfer pathway rather than from water oxidation, a decrease in oxygen evolution at the level of the PS II should appear. Thus, to investigate cyclic electron flow around PS II the decrease of oxygen production at the PS II has to be measured as described by Prasil *et al*. (1996). Such experiments can be performed with the rate electrode (see 2.5.2.2).

1.3 Aim of this Work

During this work herbicide resistant mutants, generated by Arne Materna in the framework of the EU project ‘Margenes’ were investigated. Beside genetic characterization, physiological measurements (measurements on the electron transport and investigations on oxygen evolution and photoprotective mechanisms) were done to analyse the effects of the mutations on the cells. In order to complete the genetic and physiological characterization of the mutants, preparations for gene expression analysis were performed, such as synthesis and test of hybridization probes.

2 Materials and Methods

2.1 Common Materials

All used reagents were, if not otherwise indicated, purchased from the companies Aldrich, Fluka, Merck, Riedel de Haen or Roth. Solutions and buffers were prepared using double distilled water and sterilized by autoclaving (steam pressure sterilization at 120 °C for 20 min). Non-autoclavable solutions were filtered with a 0.2 µm membrane (Roth GmbH, Karlsruhe, Germany).
Glass ware which was used for working with RNA was baked at 200 °C for 8 h while plastic ware, solutions and buffers were autoclaved twice before use. Plastic containers, the electrophoresis chamber and lid as well as the bench were cleaned with 0.1 N NaOH/ 0.1 % (w/v) SDS prior to work with RNA. Moreover, solutions and buffers were prepared with DEPC-treated water.
Centrifugation of small volumes were performed using a table-top centrifuge (model 5415D, Eppendorf, Hamburg, Germany), for large volumes and harvesting of cells the Allegra™ 25R Centrifuge from Beckman Coulter™ (Fullerton, USA) was used.

2.2 Culture Conditions

Phaeodactylum tricornutum Böhlin (University of Texas Culture Collection, strain 640) was grown photoautotrophically in 50 % (v/v) sterile natural seawater F/2 medium (Guillard and Ryther, 1962) made with Tropic Marin® (Dr. Biener GmbH, Wartenberg/Angersbach, Germany) sea salt. Liquid cultures of 200 mL were incubated at 20 °C and continuously bubbled with sterile air. The cells were illuminated at a light intensity of 45 µmol photons·m^{-2}·s^{-1} for low light (LL) or 400 µmol photons·m^{-2}·s^{-1} for high light conditions (HL) with white fluorescent tubes (Osram, München, Germany) with a 16 h light / 8 h dark cycle. Cultures were adjusted weekly to a total Chlorophyll (Chl) concentration of 0.32 µg·mL^{-1}.
For growing the algae on plates, solid medium was used containing F/2 medium, 1.2 % (w/v) Bactoagar (Becton, Dickinson & Co., Sparks, USA) and $5 \cdot 10^{-6}$ M DCMU. The plates were incubated in a culture chamber at 21 °C.

2.3 Chlorophyll Extraction

Total Chl (Chl *a* and Chl *c*) was extracted as follows: 1 mL of each culture was harvested by centrifugation (5 min, 12000 rpm) and the resulting pellet was resuspended in 100 µL methanol. 900 µL of acetone was added and the cells were broken by vortexing. After centrifugation at 12000 rpm for 10 min the supernatant was used to determine the Chl concentration by measuring the OD at 664 and 630 nm with a spectrophotometer (Ultrospec 2100 *pro* UV/Visible Spectrophotometer, Amersham Biosciences UK Limited, Buckinghamshire, England). The concentration was calculated using the formula of Jeffrey and Humphrey (1975):

$$\text{Chl } a \text{ (mg/L)} = 11.47 \cdot OD_{664} - 0.4 \cdot OD_{630}$$

$$\text{Chl } c \text{ (mg/L)} = 24.36 \cdot OD_{630} - 3.7 \cdot OD_{664}$$

2.4 Molecular Biological Methods

2.4.1 DNA Extraction

DNA from the different mutants was extracted by lysating the algae in 10 mM Tris/HCl (pH 7.5) at 96 °C for 10 min. After centrifugation for 1 min at 10000 g in a table-top centrifuge (5415 D, Eppendorf, Hamburg, Germany), the supernatant was used as template for genetic characterization of the mutants by PCR (polymerase chain reaction)

2.4.2 PCR

The sequence inbetween the nucleotide positions 1 and 1083 of the *psb*A gene was amplified by the PCR method (Saiki *et al*., 1985). The reaction was performed with Triple Master® polymerase Kit (Eppendorf, Hamburg, Germany) using the upstream primer 5'-ATGACAGCAACTTTAGAAAGACG-3' and the downstream primer 5'-ATGAAGGTATGGATTTAGTCGTGCC-3'. A PCR reaction with a total volume of 25 µL contained 1x High Fidelity buffer, 1x *Taq* Master Enhancer (both Eppendorf, Hamburg, Germany), "upstream"- and "downstream"-primer (300 µM each), nucleotide mix (MBI Fermentas, St. Leon-Rot, Germany) with a final concentration of 200 µM, template DNA (1-50 ng) and the polymerase mix (2.5 u). The amplification

was performed in a PCR cycler (TGradient, Biometra® GmbH, Göttingen, Germany) by applying the following standard program:

1. pre-denaturation:	94 °C	4 min	
2. annealing	55 °C	45 s	
3. elongation	68 °C	1 min 20 s	35x
4. denaturation	93 °C	45 s	
5. post-annealing	55°C	10 min	
6. post-elongation	68 °C	10 min	

2.4.3 Horizontal Gel Electrophoresis

PCR products were analyzed by horizontal gel electrophoresis (Sambrook *et al*., 1989). The DNA was separated in 1 % (w/v) agarose gels using a ComPhor Mini chamber purchased from Biozym Scientific GmbH (Hess/Oldendorf, Germany). Before loading the samples on the gel, the DNA was mixed with 6x loading buffer (MBI Fermentas, St. Leon-Rot, Germany). For separation a constant voltage of 85 V was applied for approx. 1 h in 1x TAE buffer [40 mM Tris/acetate (pH 8.0), 1 mM EDTA]. The DNA was stained with EtBr and visualized under UV.

For separating RNA, electrophoresis had to be performed under denaturing conditions, as single stranded RNA can form secondary structures which influence the run. The gel contained 1.2 % (w/v) Agarose, 1x MOPS buffer (20 mM MOPS, 5 mM Sodium Acetate, 1 mM EDTA, pH 7.0) and 16 % (v/v) formaldehyde. The RNA samples were mixed with self made loading dye (1x MOPS, 50 % (v/v) formamide, 16 % (v/v) formaldehyde, 10 mg/mL bromphenolblue, 3 µg/mL EtBr) and denatured at 65 °C for 10 min before separation. Separation was performed by applying a constant voltage of 45 V for 2-3 h in 1x MOPS buffer.

2.4.4 Purification of DNA

For purifying the PCR products, the Nucleo Spin® Extract Kit from Machery-Nagel (Düren, Germany) was used as described by the manufacturer. After drying the column by centrifugation an additional drying step was added. For this, the column was dried by incubation on the bench for several minutes, so that the remaining ethanol could evaporate.

2.4.5 Ligation

Purified PCR product was inserted in the plasmid vector pGEM®-T (Promega, Madison, USA) as described by the manufacturer using T4 DNA ligase. A reaction mix of 10 µL contained 1x Rapid Ligation Buffer, open vector (50 ng), DNA and T4 ligase (3 u). Open vector and DNA were added to the reaction mix in the ratio of 1:3.

2.4.6 Competent Cells and Transformation

For preparation of chemo competent *E.coli* XL 1 blue cells (Stratagene, La Jolla, USA) the protocol of Hanahan (1983) was used. A 250 ml culture which was grown in SOC-Medium (2 g/L Tryptone, 0.5 g/L Yeast Extract, 10 mM NaCl, 2.5 mM KCl, 20 mM $MgCl_2$, 20 mM Glucose) at 21 °C was harvested at an OD_{600} of about 0.5 by centrifugation (2500 g, 10 min, 4 °C). The pellet was resuspended in transformation buffer (TB; 4 °C) containing 10 mM Pipes, 55 mM $MnCl_2$, 15 mM $CaCl_2$ and 250 mM KCl and centrifuged again as described above. Finally the cells were resuspended in TB (4 °C) with 7 % (v/v) DMSO and incubated on ice for 10 min. Aliquots of 500 µL were stored at -80 °C until use.

For the transformation, the cells were thawed on ice and 5 µL of the ligation mix (see 2.4.5) were added. After incubation on ice for 10 min the cells were heat-shocked for 75 s at 42 °C. Subsequently the cells were cooled on ice and after addition of 500 µL LB (Luria-Bertani) medium (10 g/L Tryptone, 5 g/L Yeast Extract, 5 g/L NaCl) the cells were incubated at 37 °C for 1 h under constant shaking (950 rpm) in a Thermomixer (model 5450, Eppendorf, Hamburg, Germany) for phenotypical expression. Different aliquots were thereafter plated on selective LB-agar plates (LB, 15 g/L Bactoagar) and incubated at 37 °C over night.

2.4.6.1 Selection of Transformed Cells

The transformed vector contains a gene for ampicillin-resistance as well as the α-fragment of the β-galactosidase gene *lacZ* and the *lac*-promoter. Therefore LB-plates which contained 100 µg/mL ampicillin, 0.1 mM IPTG and 80 µg/mL X-Gal were used. IPTG induces the expression of the vector. Cells that did not contain the vector

couldn't survive, as the ampicillin-resistance gene is not expressed, while cells that did uptake the vector formed colonies. Since the multiple cloning site lies in the *lacZ* gene, cells containing vector without inserted DNA were coloured in blue. This is due to the fact, that β-galactosidase is expressed in these cells and reacts with X-Gal which is present in the LB-plates. During this reaction called blue-white screening (Sambrook *et al.*, 1989) the blue dye is produced.
Ampicillin resistant white colonies were transferred to liquid LB (Luria-Bertani) medium containing 100 µg/mL ampicillin and incubated at 37 °C for 12 h.

2.4.7 Plasmid Preparation

Plasmids were purified using the QIAprep® Spin Miniprep Kit (Qiagen, Hilden, Germany) as described by the manufacturer. In contrast to the given protocol an additional drying step was added after drying the column by centrifugation. Before elution the column was incubated on the bench for several minutes so that remaining ethanol could evaporate.
DNA concentration was measured with a spectrophotometer by using following formula:

$$C_{DNA} = OD_{260} \times DF \times MF$$

with DF = dilution factor and MF = DNA specific multiplication factor (= 50 for DNA).
DNA purity was estimated by the ratio of OD_{260}/OD_{280}, which should be between 1.8 and 2.0.

2.4.8 Sequencing

Sequencing was performed at Sequiserve (Vaterstetten, Germany). For analysis of the sequences the Lasergene® Software (DNASTAR Inc., Madison, USA) was used.

2.4.9 Protein Extraction

For protein extraction cells were harvested in exponential phase of growth by centrifugation at 3000 g for 10 min and crushed under liquid nitrogen with mortar and pistil. The broken cells were solubilized in preheated (60 °C) extraction buffer containing 125 mM Tris/HCl (pH 6.8), 4 % (w/v) SDS, 200 µM PMSF and 100 mM

DTT. The solution was incubated at 100 °C for 10 min and centrifuged for 15 min at 16000 g in a table-top centrifuge at room temperature. The supernatant was then mixed with four volumes of acetone (4 °C) and protein precipitated by incubation at -20 °C for at least 1 h. After centrifugation (4000 – 5000 g, 10 min, 4 °C) the protein pellet was washed with 70 % (v/v) ethanol (4 °C) and centrifuged again as above. The dried pellet was finally resuspended in extraction buffer.
Protein concentration was estimated by using the Bradford (1976) method (BCA™ Protein Assay Kit, Pierce, Rockford, USA).

2.4.10 SDS – PAGE

Total protein was normalized to equal amounts of Chl a, mixed with the appropriate amount of 5x SDS sample buffer [125 mM Tris/HCl (pH 8), 10 % (w/v) SDS, 25 % (v/v) glycerol, 25 % (v/v) β-mercaptoethanol, 0.025 % (w/v) bromphenolblue] and denatured by incubation at 95 °C for 5 min. SDS – PAGE was carried out using the buffer system established by Laemmli (1970). Electrophoresis was performed using a 12 % (w/v) polyacrylamide separating gel and a 5% (w/v) stacking gel:

- stacking gel: acrylamide [30 % (w/v)], 300 mM Tris/H_3PO_4 (pH 6.7), 0.5 % (w/v) SDS, 0.1 % (v/v) TEMED, 0.15 % (w/v) APS.
- separating gel: acrylamide [30 % (w/v)], 1.875 M Tris/HCl (pH 8.9), 0.25 % (w/v) SDS, 0.05 % (v/v) TEMED, 0.07 % (w/v) APS.

Separation of the proteins was performed by applying a constant voltage of 100 V for 1 – 1.5 h in a buffer containing 0.25 M Tris, 1.92 M Glycine and 0.5 % (w/v) SDS.

2.4.11 Western Blot

The proteins separated by SDS – PAGE were transferred electrophoretically on a PVDF membrane (Hybond™-P, Amersham Biosciences UK Limited, Buckinghamshire, England) using a semidry electroblotter (Fastblot B32, Biometra® GmbH, Göttingen, Germany) at a constant current of 0.8 mA cm^{-2} for 1.5 h. Transferred proteins were blocked in Phosphate-buffered saline [PBS: 137 mM NaCl, 2.7 mM KCl, 8 mM Na_2HPO_4, 1.8 mM KH_2PO_4 and 0.02 % (v/v) Tween 20; pH 7.4] with 5 % (w/v) fat-free milk powder for 1 h. The membrane was then incubated with the first antibody against D1 overnight at 8 °C. The Anti-D1 serum provided by

AgriSera (Vännäs, Sweden) was diluted 1:4000 in PBS with 5 % (w/v) fat-free milk powder. After several washings with PBS the membrane was incubated for 1.5 h with goat-anti-rabbit-IgG-peroxidase conjugate [diluted 1:10000 in PBS with 5 % (w/v) fat-free milk powder] purchased from Sigma (München, Germany) and subsequently washed for several times in PBS. Detection was performed using the enhanced chemiluminescent (ECL) detection system [BM Chemiluminescence Blotting Substrate (POD), Roche Diagnostics GmbH, Mannheim, Germany] and X-ray films (Hyperfilm™ ECL, Amersham Biosciences UK Limited, Buckinghamshire, England). To prove blotting efficiency, membranes were stained with Amido Black (Sambrook *et al*., 1989) after the ECL reaction.

2.4.12 Southern Blot

The main purpose of the Southern Blot (Southern, 1975) is to fix DNA fragments which were separated by electrophoresis on a membrane and to detect specific fragments by hybridization with labeled probes.

For the experiments, *Sca*I digested total DNA was separated by horizontal gel electrophoresis as described above. The gel was then incubated in 250 mM HCl for 10 min for partial depurination of the DNA. To denature the DNA, the gel was incubated in a solution containing 0.5 M NaOH and 1.5 M NaCl for 15 min and subsequently neutralized for 15 min in 0,5 M Tris/HCl (pH 7.0)/1.5 M NaCl. For transferring the DNA on the membrane (Nytran® SuPerCharge nylon membrane, Whatman®, Middlesex, UK) the TurboBlotter™ system provided by Schleicher & Schuell (Dassel, Germany) was used according to the manufacturer's instructions. Basically a high-salt buffer [here: 20x SSC (pH 7.0), containing 3 M NaCl, 0.3 M NaCitrate] is absorbed by a pile of dry paper towels through the gel and the membrane due to capillary forces. The DNA migrates with the buffer and is stopped by positively charged membrane.

The DNA was fixed to the membrane by UV cross-linking. For this the membrane was irradiated with 0.12 J cm^{-2} of UV light using a cross linker (model Stratalinker®) by Stratagene (La Jolla, USA). After several washing steps in 5x SSC and 2x SSC to reduce the salt concentration, the membrane was blocked in High SDS buffer [5x SSC, 7 % (w/v) SDS, 2 % (w/v) blocking reagent (Roche Diagnostics GmbH, Mannheim, Germany), 50 mM NaH_2PO_4 (pH 7.0), 0.1 % (w/v) N-Lauroylsarcosine,

50 % (v/v) formamide] for 1h at 42 °C in a hybridization oven (Biometra® GmbH, Göttingen, Germany). Hybridization was carried out overnight at 42 °C in High SDS buffer containing the DIG-labeled probe. The membrane was washed several times in 2x SSC/0,1 % (w/v) SDS, incubated two times in 0.5x SSC/0.1 % (w/v) SDS at 65 °C for 15 min and blocked in blocking buffer (1x blocking reagent in 100 mM maleic acid). Incubation with the antibody against DIG (digoxigenin) was performed at room temperature for 30 min. The antibody (α-DIG, Roche Diagnostics GmbH, Mannheim, Germany) was diluted 1:20000 in blocking buffer. After washing the membrane three times in 100 mM maleic acid/0.3 % (v/v) Tween 20 for 20 min detection was performed by incubating the membrane in detection buffer (0.1 M Tris/HCl, 0.1 M NaOH, pH 9.5) and CDP *Star* ready-to-use(Roche Diagnostics GmbH, Mannheim, Germany). Chemiluminescence was recorded on X-ray films.

2.4.13 RNA Extraction

The cells were harvested in exponential phase of growth, centrifuged at 1000 g for 5 min at 4 °C and crushed under liquid nitrogen with RNase-free mortar and pistil. For extracting RNA the RNeasy® Protect Starter Kit provided by Qiagen (Hilden, Germany) was used and extraction performed as described by the manufacturer.

2.4.14 cDNA Production

For preparing cDNA of RNA the Reverse Transcription System from Promega (Madison, USA) was used. The reaction mix contained: 5 mM $MgCl_2$, 1x reverse transcription buffer, 2 mM nucleotide mix, 100 µg/mL oligo (dT), 3 µg RNA, 20 u RNAsin and 18 u reverse transcriptase. After incubation at 42 °C for 30 min, the reaction was stopped at 95 °C for 5 min and cooled on ice before storage at -20 °C. RNA was denatured at 70 °C for 10 min prior to the reaction.

2.4.15 DIG-labeled Hybridization Probes

Primers for synthesising probes were derived from EST sequences and were 20 – 30 bp long. Synthesis of the oligonucleotides was performed by Operon Biotechnologies GmbH (Köln, Germany).

primer	sequence 5' - 3'	binds in	product length
P-rps4-5' P-rps4-3'	ATATGTAAAAGAAGCACGCCG AAGTTGTAAGGATACATCATTCCG	*rps*4	364 bp
P-hliB-5' P-hliB-3'	AATCGGGACGCGTCGGTGGGAGGC AAGTTTGCTGGTTTCGCAGTCGGG	*hli*B	484 bp
P-hliA-5' P-hliA-3'	TCGTGTCAGTGGTCGCCGCATATCCTAACGG AGCTATTTGTTTAGAATCCAAATTCGGGGC	*hli*A	614 bp
P-fcpA-5' P-fcpA-3'	CGTTTTTGCCTCCCTCCTCGCC GAGAGCAAGGATGCCCATTTGTGCCGC	*fcp*A	541 bp
P-DDE-5' P-DDE-3'	GCATTGGCACTAACGATTGGTGTCGC TTGTCGTGGTTGATCAAGTGACCCG	*DDE*	584 bp
P-Actin-5' P-Actin-3'	GATACGCCCTTCCGCACGCCGGAT CTGGAAGGTCGAAAGCGAGGCG	actin	557 bp
P-18S rRNA-5' P-18S rRNA-3'	AGCTCGTAGTTGGATTTGTGGTGGC TCCCGTGTTGAGTCAAATTAAGCCGC	18S rRNA	580 bp

***Table 2.1*: Used Primers for Synthesis of DIG-labeled Probes.** Name and sequence of the primers are shown, as well as the genes wherein the primers bind and the estimated length of the PCR product.

The primers were tested by PCR using the *Taq* DNA polymerase (Eppendorf, Hamburg, Germany) and then used for synthesis of the DIG-labeled probes. The reaction mix for DIG-labelling contained 1x *Taq* buffer, 1x *Taq* Master Enhancer (both from Eppendorf, Hamburg, Germany), DIG-labeled nucleotides (PCR DIG probe synthesis mix from Roche Diagnostics GmbH, Mannheim, Germany), “upstream”- and “downstream”-primer (300 µM of each), 10 – 50 ng total DNA as template and *Taq* DNA polymerase (2.5 u). The amplification was performed by using following program:

1. pre-denaturation:	95 °C	3 min	
2. annealing	61 °C	1 min	↰
3. elongation	72 °C	3 min	30x
4. denaturation	95 °C	30 s	
5. post-annealing	58°C	10 min	
6. post-elongation	72 °C	10 min	

Analysis of the PCR products by gel electrophoresis and purification of the DNA was performed as described above whereas attention has to be paid, as the bands appear longer as they are in reality, which is due to the digoxigenin labels, which are increasing the size of the fragments.

2.4.16 Dot Blot

For quantifying the probes the Dot Blot method was used (Kafatos *et al.*, 1979). For this, different dilutions of DIG labeled control DNA, with known concentration and the probes were made in detection buffer (0.1 M Tris/HCl, 0.1 M NaCl, pH 9.5) containing salmon sperm DNA (50 µg/mL). 1 µL of each sample was applied on a positively charged nylon membrane and DNA was fixed to the membrane by UV cross-linking (see 2.4.12). After incubation in maleic acid buffer (100 mM maleic acid, 150 mM NaCl, pH 7.5) the membrane was blocked in blocking solution [1 % (w/v) blocking reagent in maleic acid buffer] and incubated with an antibody against digoxigenin (diluted 1:10000 in 100 mM maleic acid) for 30 min. The membrane was washed twice in maleic acid buffer with 0.3 % Tween 20 for 15 min and then incubated in detection buffer for 5 – 10 min. Detection was performed by incubation in detection buffer with NBT/BCIP ready-to-use (Roche Diagnostics GmbH, Mannheim, Germany).

2.4.17 Northern Blot

After separation of the RNA by denaturing gel electrophoresis as described above, the RNA was transferred on a nylon membrane as described in 2.4.13. After cross-linking and washing in 2x SSC, pre-hybridization followed for 3-4 h at 42 °C in High-SDS buffer. For hybridization 500 – 800 ng of the DIG-labeled probe were denatured at 96 °C for 10 min and added to 20 mL High-SDS buffer (68 °C). The probe/High-SDS buffer mix was then added to the membrane and incubated over-night at 42 °C. After two washing steps in 2x SSC/0.1 % (w/v) SDS for 10 min at room temperature, the membrane was washed in 0.5x SSC/0.1 % (w/v) SDS for 15 min at 65 °C twice and subsequently incubated in maleic acid buffer (100 mM maleic acid, 150 mM NaCl, pH 7.5) with 0.3 % (v/v) Tween 20 for 2 min. The membrane was blocked in blocking buffer [1 % (w/v) blocking reagent in maleic acid buffer] for 1 h at room temperature and incubated with an antibody against DIG (diluted 1:20000 in blocking buffer) for 30 min at room temperature. Washing was performed twice in maleic acid buffer supplied with 0.3 % (w/v) Tween 20 for 15 min before detection of the antibody was carried out as described in 2.4.13.

2.5 Photosynthetic Activity Measurements

2.5.1 Chlorophyll Fluorescence Emission

2.5.1.1 Conventional Fluorometer

The fluorometer used in this work is a homemade apparatus which was developed in 2001 at the ENS Paris (Parésys *et al*., 2005).

The system consists of three parts (Fig. 2.1):

1. A data acquisition card (PCL 818, Advantech, Canada) inserted in a computer together with the software which allows writing protocols of macroinstructions to control the lighting events such as the light intensity, color of light, duration of illumination and sensitivity of the photomultiplier.
2. The electronic devices and
3. a detector unit [Fig. 2.1(b)]. It includes a compartment containing the sample illuminated from three sides by blue, red and green light. The sample compartment is isolated from ambient light by a cap. On the fourth side, chlorophyll fluorescence is detected by a miniature photomultiplier module (PM) (H5701-50, Hamamatsu, Japan) together with an amplifier and a high voltage supply. The PM is protected by an interference filter (S10 680 F, Corion, USA) which allows detection at 680±10 nm. Each light source consists of an array of six light emitting diodes (LED) and a specific interference filter combination.

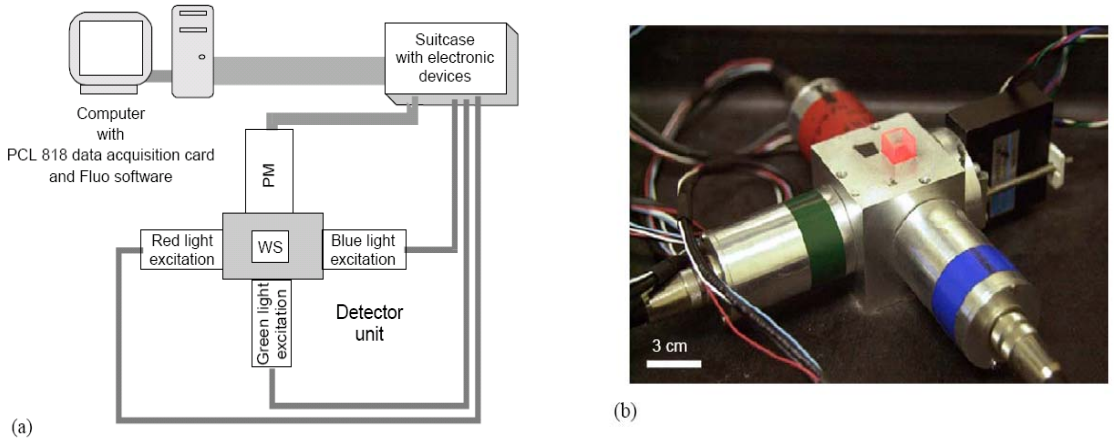

***Fig. 2.1*: a) Schematic Presentation of the Fluorometer.** PM: photomultiplier, WS: water sample. **b) Picture of the Detector Unit with the Cuvette illuminated with red Light** (Parésys *et al*., 2005).

Different phases which refer to the redox state of the different electron carriers from PS II to PS I (so-called fluorescence induction kinetics) can be measured, as shown in Fig. 2.2. F_0 is the minimal fluorescence yield of dark-adapted cells and F_m is the maximal fluorescence reached during light exposure. F_v is the variable fluorescence and is calculated as F_m minus F_0.

The extent of the rise from F_0 to F_i is a global measurement of the reduction of the first quinone (Q_A) lying downstream of the PS II reaction center, while the ratio F_v/F_m is considered to be an indicator of the photosynthetic capacity (Krause and Weis, 1991).

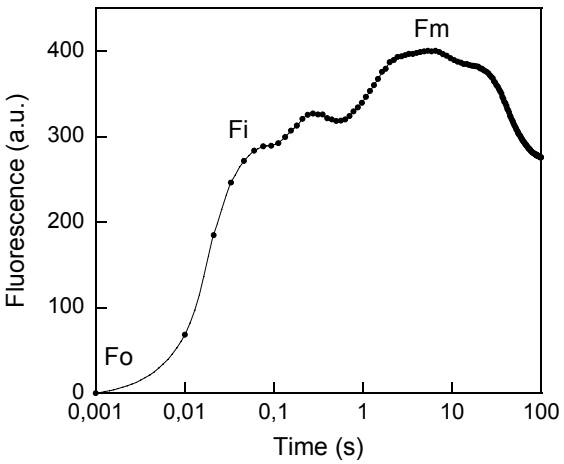

***Fig. 2.2*: Different Levels of Chlorophyll Fluorescence Emission of WT Cells measured with a conventional Fluorometer.** F_0: minimal level of fluorescence, normalized to 0, F_m: maximal level of fluorescence.

For all kind of measurement, the following procedure has been used. The algae samples were adjusted to a final Chl *a* concentration of 20 $\mu g \cdot L^{-1}$ and dark-adapted for 20 min. The samples were held in cuvettes (ref. 613101, Greiner, Germany) that were shaken just before the start of the experiment to resuspend the cells that had settled. Measurements were done in three replicates for each sample. The illumination sequence was first done on a blank of medium and then on the algae sample. At the end, the signal from the blank was subtracted and the values were averaged.

Three measurements were performed:

1) The fluorescence induction kinetics to quantify the rise F_0 to F_i. They were recorded for red light only (it emits the highest light intensity) using different light intensities, whereas a new sample was used for every intensity.

2) Resistance to DCMU. Different concentrations of the herbicide (final concentration: 10^{-9} M – saturated) were added to the blank and samples after 20 min dark-adaptation. The samples were then incubated in the dark for another 15 min before the measurement. The extent of the rise F_0-F_i was used has an indicator of the inhibition of the PSII activity by DCMU.
3) F_v/F_m was measured by using a protocol written by Dr. Johann Lavaud. A mix of blue and red lights was used to obtain a light intensity as high as the fluorometer can provide while keeping the noise of the signal constant. The protocol consisted in a series of short pulses of different colour and intensity: a blue light pulse of low intensity followed by a red light pulse of low intensity. Those two pulses were used to asses the F_0 level. The F_m level was measured by giving a mix of blue and red light pulses of strong intensities. The series was consecutively applied three times to the blank to get a precise measurement of the background signal, and one time to the cells.

2.5.1.2 Modulated Fluorometer

A Pulse Amplitude Modulated (PAM) fluorometer (PAM IMAG-K, Walz, Effeltrich, Germany) (Schreiber *et al*., 1986) was used to measure NPQ (non-photochemical fluorescence quenching). The main difference in comparison to a conventional system is that with a modulated fluorometer the light source used to measure fluorescence is, as the name says, modulated. This means that the light is switched on and off at high frequency while the detector is tuned to detect only fluorescence excited by the measuring light. Therefore the relative yield of fluorescence can now be measured in the presence of background illumination which intensity can be changed without influencing the fluorescence signal detection as for a conventional fluorometer.

As shown in Fig. 2.3 the measurement is initiated by switching on the measuring light, giving a measure of the F_0 (minimal) level of fluorescence. A saturating flash of light is then applied, allowing the measurement of F_m in the dark-adapted state. Following on from this, an actinic light is applied and at appropriate intervals, further saturating flashes are applied. From each of these, a value for F_m', the fluorescence maximum in the light, can be measured. The steady state value of fluorescence

immediately prior to the flash is termed F_t (not shown in figure). After a flash, removal of actinic light allows measurement of F_0'.

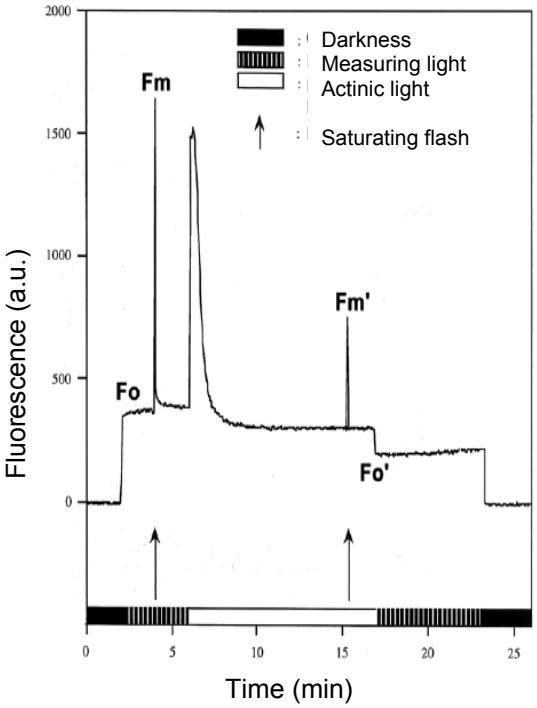

***Fig. 2.3*: Sequence of a typical Fluorescence Trace.** When the measuring light is switched on the zero fluorescence level is measured (F_0). Application of a saturating flash of light allows measurement of the maximal fluorescence level F_m. A light to drive photosynthesis is then applied (actinic light) and after a period of time another saturating light flash allows the maximum fluorescence in the light (F_m') to be measured. Turning of the actinic light allows the zero level of fluorescence (F_0') in the light to be estimated.

With the different fluorescence levels that can be measured, several fluorescence parameters such as NPQ can be evaluated:

$$NPQ = (F_m - F_m')/F_m'$$

NPQ is a parameter which evaluates the extent of the energy dissipation of the excitation energy in excess in the antenna of PSII. This process participates to global photoprotection.

2.5.2 Photosynthetic Oxygen Emission

2.5.2.1 Clark Electrode

The oxygen electrode used is a Clark Electrode (Clark, 1956) based on a design by Delieu and Walker (1981) which allows measurement of the oxygen concentration in the algae suspension. The sensor consists of a platinum cathode and a silver anode which are set in an epoxy resin disc with the cathode at the centre of a dome which is

surrounded by the anode set into a well which also serves as the electrolyte reservoir [Fig. 2.4 (a)].

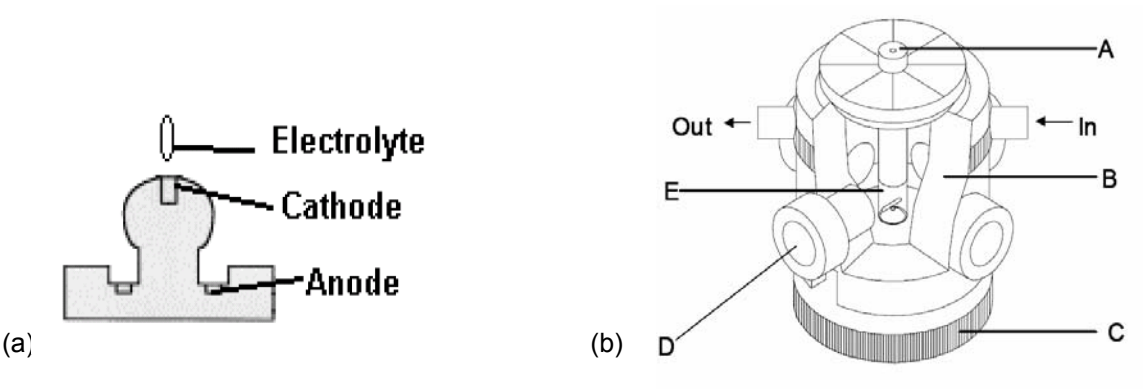

***Fig. 2.4*: (a) The oxygen sensor,** with the platinum cathode at the centre of a dome surrounded by a well which contains the silver anode. The electrolyte is placed on the top of the dome. (**b) Cut-away view of the electrode unit.** The tight-fitting plunger, nut and cap (A), water jacket (B) and base (C) are manufactured from black acetal to exclude light. Optical equipment may be inserted into each of the four optical ports (D) which are located at right angles to one another around the reaction chamber (E) where the algae cells are incubated. At the bottom of the reaction chamber the oxygen sensor described in (a) is found. Temperature control can be provided by circulating coolant through the water jacket. The coolant inlet and outlet connections are also shown by the "In" and "Out" arrows (Figure from Hansatech Instruments Limited, 2000).

The electrolyte bridge between the anode and cathode is established by placing a drop of electrolyte (here 50 % KCl solution) on top of the dome.

Application of a stable polarising voltage (around 700 mV) initiates electrochemistry in the sensor where the silver anode reacts with the anions in the electrolyte. In the case of KCl electrolyte, silver chloride is produced with the release of electrons (equation 1), which are used at the platinum cathode to catalyse the reduction of oxygen (equation 2):

Equation 1: $Ag \rightarrow Ag^+ + e^-$ followed by: $Ag^+ + Cl^- \rightarrow AgCl$

Equation 2: $O_2 + 2H_2O + 2e^- \rightarrow H_2O_2 + 2OH^-$ followed by $H_2O_2 + 2e^- \rightarrow 2OH^-$

The oxygen molecules reach the cathode via a PTFE membrane which is impermeable for water and ions. The magnitude of the current flow produced is related to the consumption of oxygen at the cathode which in turn is determined by the concentration of dissolved oxygen present in the electrolyte which is proportional to the oxygen concentration of the surrounding media.

With this method, change of oxygen concentration due to photosynthesis and respiration can be measured, giving information about the global photosynthetic activity of the algae which are held in the reaction chamber. Under illumination with changing light the amount of emitted oxygen is a function of the different intensities. This allows us to build curves of the oxygen evolution as a function of the light intensity (P-E curves) which are used for describing different parameters such as the maximum photosynthetic capacity and the light intensity for which the oxygen emission is saturated.

For this experiment a special electrode system was used (DW 2/2; Hansatech Instruments Ltd., Norfolk, England) which allows measurements in the dark because of a water jacket which is made of black acetal [Fig. 2.4 (b)]. Before each experiment the electrode was calibrated with sodium dithionite and oxygen saturated water from 0 % to 100 % respectively. The algae (grown under LL) were harvested during the exponential phase of growth, centrifuged at 1500 rpm for 5 min and resuspended in their culture medium to a final Chl *a* concentration of 8 $\mu g \cdot mL^{-1}$. The cells were kept under low light at 20 °C under regular shaking for at least 1 h for recovering. Samples of 1.5 mL were dark adapted for 15 min followed by illumination during 5 min at various intensities. White light of adjustable intensity (measured with LI 185A, LI-COR® Inc., Lincoln, USA) was provided by a KL 1500 quartz iodine lamp (Schott, Mainz, Germany). Before each measurement 4 mM sodium bicarbonate was added to prevent any carbon limitation in the medium. A new sample was used for each light intensity.

2.5.2.2 Rate Electrode

The rate electrode established by Joliot (1968) has such a high resolution (it responds during milliseconds of time) that it is able to measure the oxygen sequence corresponding to different oxidation states of the oxygen evolving complex (OEC) (Fig. 1.2). The experimental procedure used here was first described by Lemasson and Etienne (1975) (Fig. 2.5). The algae are lying in a monolayer and therefore have a direct contact with the platinum electrode and cover its whole surface. The cells are maintained in this position with a dialysis membrane. Above, medium circulates to guarantee constant oxygen concentration at the level of the membrane. A concentration gradient develops between the surface of the membrane and the

platinum electrode, where it is zero until oxygen is emitted by the cells and reduced by the electrode. Thus, the rate of oxygen emission is measured.

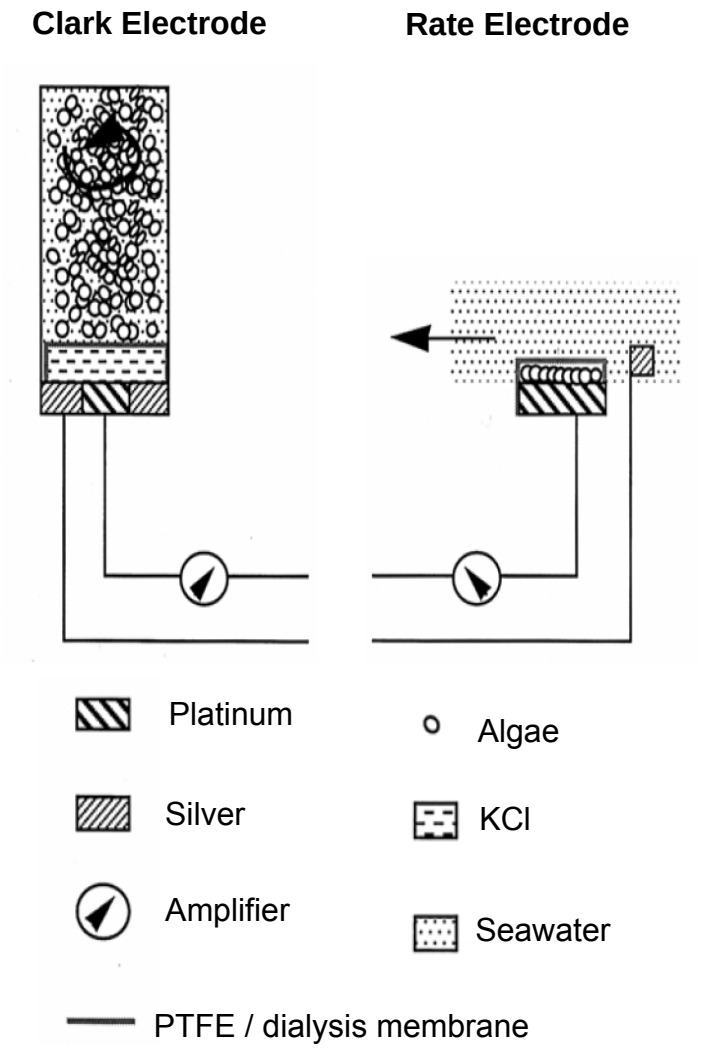

***Fig. 2.5*: Comparison of the two oxygen electrodes used** (Lavaud, 2002).

The saturating flashes used to drive the Kok cycle last for 10 µs and are separated by 500 ms from each other. They are produced by a lamp (Strobotac, General Radio Co. Concord, MA, USA) and are single turn over flashes. Their briefness and intensity are selected in a way, that every PS II receives only one electron (single hit), so that every S-state of the OEC corresponds to the absorption of one single electron (so called “single turn-over”). The quantity of evolved oxygen is maximal after the third flash, with repeated maxima after successive four flash intervals (Fig. 2.6). This is a consequence of the fact that S_1 is the dark-stable state (Fig. 1.2). Although the electronic flashes last for only few microseconds, some PS II can catch a second photon within the same flash (double hit) which results in the advance of two steps in the S-state cycle. On the contrary some PS II are not able to catch a single photon

during a flash (miss). As a consequence of a mix of single and double hits as well as misses, the oscillation is damped to a constant steady state yield, Y_{SS}, after about 20 flashes. Y_{SS} is the number of active (oxygen evolving) PS II.

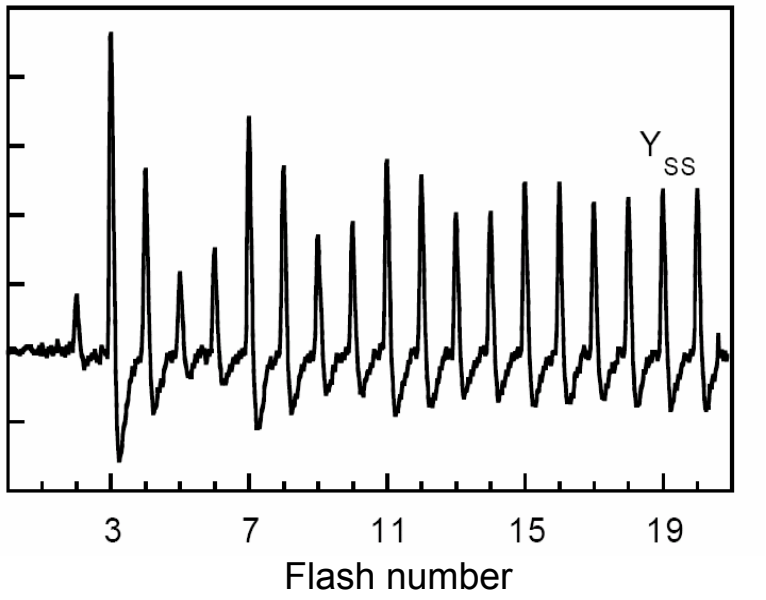

***Fig. 2.6*: Example for a signal of oxygen emission (oxygen sequence) obtained from dark-adapted *Phaeodactylum tricornutum* cells** (Lavaud, 2002).

For the experiments, cells which were grown under low light were harvested in the exponential phase, resuspended in their culture medium at 11 µg Chl a·mL^{-1} and kept under low light for recovering until use. For measuring the amount of PS II, samples of 200 µL were directly applied on the platinum electrode and covered by the dialysis membrane. For the antenna size measurements different neutral filters were placed between the light source and the algae to decrease the flash light intensities. For the photoinhibition kinetics (which is adequate to loss of PS II activity as a function of light), samples of 1.4 mL were dark adapted for 15 min in the reaction chamber of the Clark electrode. After 10 min, 200 µL were taken for a dark control measurement. The remaining algae suspension was illuminated for 5 min with different light intensities with the same lamp used for the P-E curves (see 2.5.2.1). A sample of 200 µL was taken for measurement with the rate electrode. For each light intensity a new sample of algae was used. The O_2 deficit, as defined by Lavaud *et al*. (2002) (a measurement of the PSII electron cycle) was quantified as:

$$O_2 \text{ deficit} = [20 \cdot Y_{SS}(L) - \Sigma (Y_1(L), Y_{20}(L))] - [20 \cdot Y_{SS}(D) - \Sigma (Y_1(D), Y_{20}(D))] / Y_{SS}(D)$$

With: Y_{SS}:steady-state oxygen yield, Y_x: oxygen yield at flash number x, , (L): light, (D): dark.

At each experiment the cells were incubated for 7 min on the electrode to allow the cells to settle down, before applying the flashes.

3 Results

3.1 Localization of the Mutations in the D1 Protein

To localize the positions of the mutations, a 1083 basepairs (bp) long fragment of the *psb*A gene was amplified by PCR (see 2.4.2) and the products were verified by horizontal gel electrophoresis (Fig. 3.1).

***Fig. 3.1*: Amplification of *psb*A.** Separation by horizontal gel electrophoresis.

The purified products were ligated into the target vector (pGEM-T) which could be done directly as the polymerase (Triple Master) creates an A overhang which allows annealing with the T overhang present in the vector. After successful transformation of the ligated vector in *E. coli*, positive clones were selected and verified by sequencing. The obtained sequences were aligned with the wild-type sequence. Four different mutants were found as shown in table 3.1.

Strain	*psb*A Sequence	Amino Acid Change	AA Position	Nucleotide Position
WT	…tta GTA act…			
VI-219	…tta ATA act…	Val → Ile	219	655
WT	…tac TTT ggt…			
FI-255	…tac ATT ggt…	Phe → Ile	255	763
WT	…gct TCA ttc…			
SA-264	…gct GCA ttc…	Ser → Ala	264	790
WT	…ttc TTA gct…			
LW-275	…ttc TGG gct…	Leu → Trp	275	824, 825

***Table 3.1*: *psb*A Mutations in different Mutants of *Phaeodactylum tricornutum*.** Name of the mutants are given, as well as the sequences around the mutations, amino acid changes and the positions of the mutations. Val: Valin, Ile: Isoleucin, Phe: Phenylalanin, Ser: Serin, Ala: Alanin, Leu: Leucin, Trp: Tryptophan.

In addition the guanine – adenine exchange at nucleotide position 655, also a thymin – adenine exchange at position 763, a thymin – guanine exchange at position 790 and an exchange from thymin and adenine at the nucleotide positions 824 and 825 to guanine and guanine were identified. All four point mutations led to single amino acid exchanges altering the D1 protein sequence from Valine to Isoleucine at amino acid

position 219 (VI-219), from Phenylalanine to Isoleucine at position 255 (FI-255), from Serine to Alanine at position 264 (SA-264) and from Leucine to Tryptophan at amino acid position 275 (LW-275). The mutation at the amino acid position 219 (VI-219) is located in the transmembrane α-helix D of the D1 protein, while the mutation found at position 255 (FI-255) lies in an α-helix close to the Q_B pocket. The mutation at position 264 (SA-264) is located within the Q_B pocket. In the α-helix E, the mutation at position 275 (LT-275) is found. This mutation is located close to a histidine which is involved in the binding of a non-heme iron (Fig. 3.2).

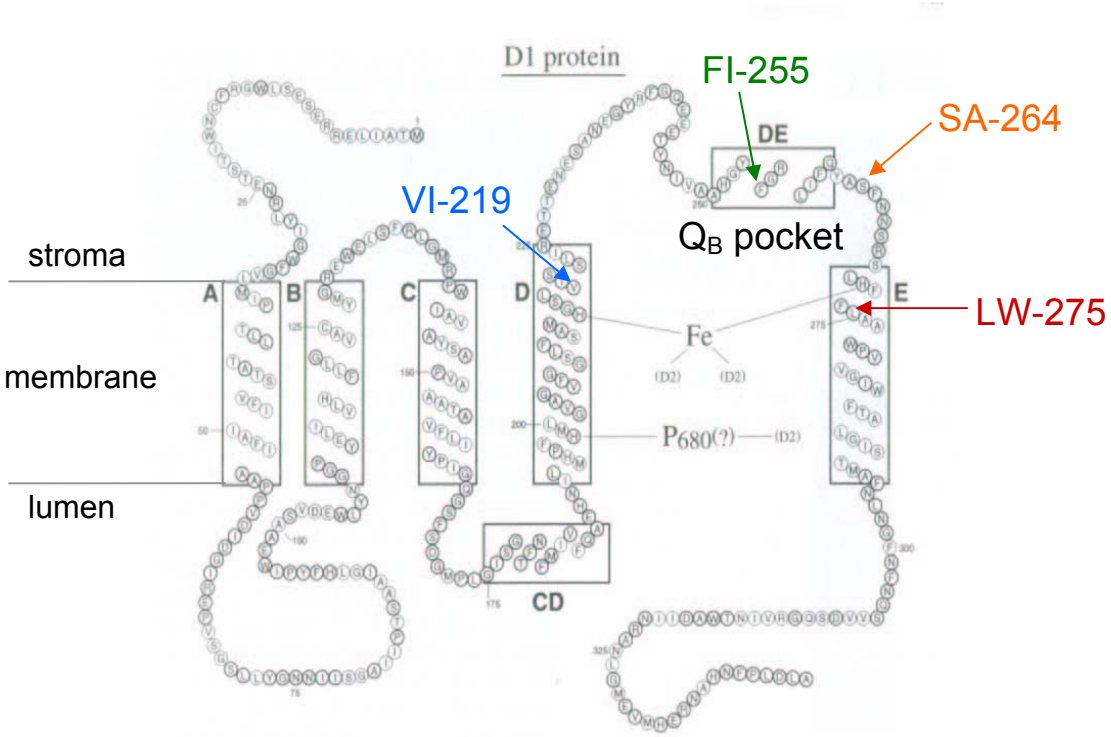

***Fig. 3.2*: Secondary Structure Profile of the D1 Protein.** α-helices are boxed and indicated by letters. A, B, C, D and E are transmembrane α-helices. Positions of the four mutations are indicated by arrows. Localization of the Q_B binding niche is also given.

3.2 Growth and Photosynthetic Capacity of the Mutants and WT

Mutations at the same positions within the *psb*A have already been described in green algae (Erickson et al., 1989) and were shown to affect the electron transport from Q_A to Q_B and consequently photosynthesis and growth. Therefore growth of the different mutants under low light conditions and the photosynthetic capacity of the cells were examined. The cultures were adjusted weekly to a total Chlorophyll (Chl *a* +Chl *c*) concentration of 0.32 $\mu g \cdot mL^{-1}$. Subsequently samples were taken daily and used for growth curves experiments by measuring the amount of Chl *a* as an

indicator of biomass (see 2.3). Further the photosynthetic capacity F_v/F_m was determined.

For the growth curves the averaged values from several measurements were plotted as a function of time. As shown in figure 3.3. VI-219 was growing like wild-type while in the exponential phase of growth FI-255 and SA-264 started with a delay of one day, but reached the same final biomass level of approximately 9 $mg \cdot L^{-1}$ at stationary phase. The growth rate of these four strains was similar (2.7 x per day). LW-275 grew slower than WT or the other mutants, also showing a delay of the exponential phase of one day like FI-255 and SA-264. In addition a lower growth rate of about 1.92 $x \cdot day^{-1}$ was found which is only 72 % of the growth rate of the other cultures. For that reason the mutant only had a final biomass level of about 6 $mg \cdot L^{-1}$ Chl *a*.

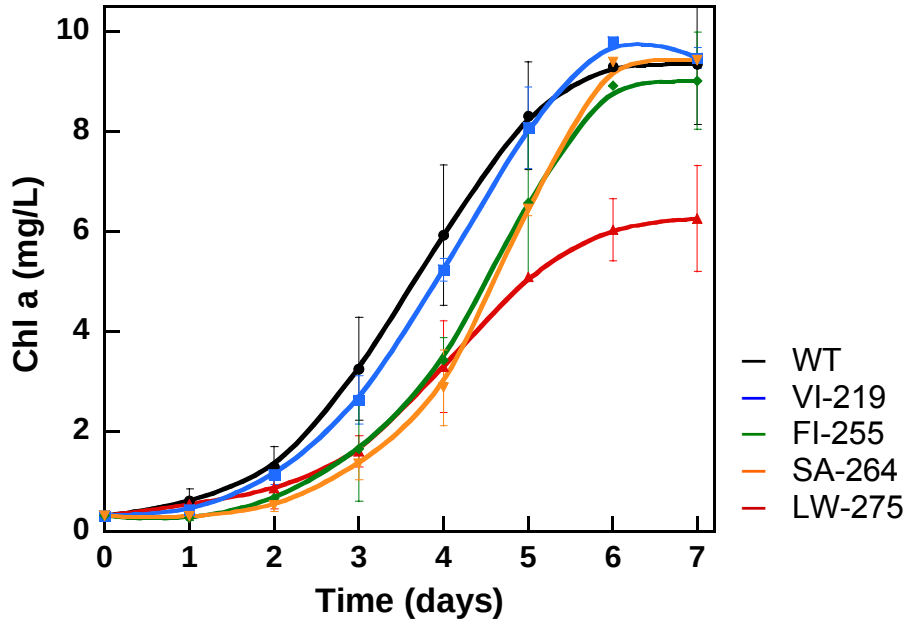

***Fig 3.3*: Growth Curves of the different Mutants under low Light (45 µmol photons·m^{-2}·s^{-1}).** WT curve is in black, VI-219 in blue, FI-255 in green, SA-264 in orange and LW-275 in red.

To investigate the maximal photosynthetic capacity, F_v/F_m was measured. When a leaf or algal cells are transferred from darkness to light usually an increase in the yield of chlorophyll fluorescence is observed. This is a consequence of a reduction of electron acceptors in the photosynthetic pathway, in particular Q_A. Once PS II absorbs light and Q_A has accepted an electron, it is not able to accept another until it has passed the first onto a subsequent electron carrier (Q_B). During this period, the reaction center is said to be 'closed'. At this stage chlorophyll fluorescence is

maximal (F_m). By measuring the basic fluorescence of photosynthetic material in the dark the minimal level of fluorescence F_0 is obtained. F_v is the variable fluorescence which is the difference of F_m and F_0 (= minimal level of chlorophyll fluorescence). For F_v/F_m the F_v value is divided by F_m.

The ratio F_v/F_m is considered to be an indicator of the photosynthetic capacity (Krause and Weis, 1991) and also reflects the global physiological status of the cells.

For the experiment the cells were adjusted to a final Chl *a* concentration of 20 $\mu g \cdot L^{-1}$ and dark-adapted for 20 min. The samples were shaken just before the start of the experiment to resuspend the cells. A protocol was used to measure F_v/F_m (for details of the protocol see 2.5.1.1)

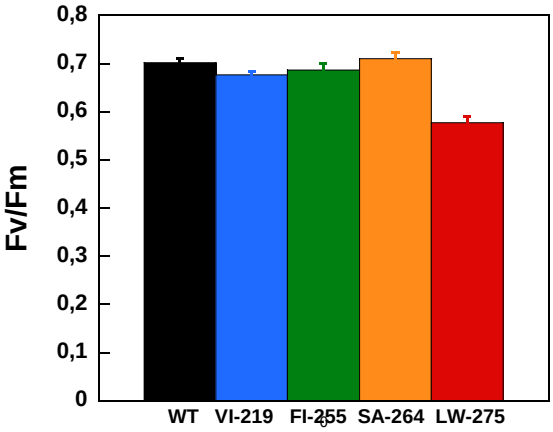

***Fig. 3.4*: Maximal photosynthetic Capacities of the Mutants in Comparison to the WT.** Values are for cells in exponential phase of growth. Standard deviation was calculated from a total of 3 experiments.

F_v/F_m is the same for WT, SA-264, FI-255 and VI-219 and about 82 % of the value of WT for LW-275 (Fig. 3.4). For diatoms, values around 0.7 are usually found during exponential growth, which is the case for WT, VI-219, FI-255 and SA-264. Values lower than this are usually seen when the organism is exposed to stress, indicating in particular the phenomenon of photoinhibition. This might be the case for LW-275 where the average F_v/F_m is 0.57.

3.3 Electron Transport

3.3.1 DCMU Resistance

Many herbicides that inhibit electron transfer from Q_A to Q_B bind to D1, thereby displacing Q_B from its binding niche (Tischer and Strotmann, 1977). It was shown, that in green algae a number of mutations in the *psb*A gene are located between the

amino acid residues 211 and 275 of the polypeptide, leading to herbicide resistance (reviewed by Erickson *et al*., 1989).

To investigate the resistance of the *psb*A mutants of *Phaeodactylum tricornutum* against DCMU the extent of the Q_A reduction in presence of different concentrations of the herbicide was measured.

When Q_B is replaced by DCMU the electron transfer from Q_A to Q_B is inhibited as Q_B cannot bind to the binding niche. Q_A remains reduced and inactivates the PS II reaction centre. The larger the extent of the rise of F_0 to F_i (see figure 2.2) the more Q_A is reduced and the more PS II is inactivated. The amount of inactivated PS II in % was plotted against the DCMU concentration (Fig 3.5).

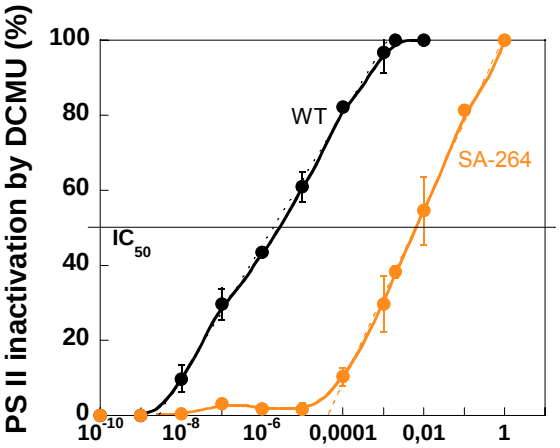

(a)

Strain	*IC_{50} (M)*	*Resistance factor*
WT	$2 \cdot 10^{-6}$	/
VI-219	$5.8 \cdot 10^{-6}$	3
FI-255	$3 \cdot 10^{-4}$	150
SA-264	$6 \cdot 10^{-3}$	3000
LW-275	$1 \cdot 10^{-3}$	500

(b)

***Fig 3.5*: Resistance to DCMU. (a)** Example for a plot, showing the inactivation of PS II by DCMU in % for the WT and SA-264. **(b)** Table showing the IC_{50} in M and the resistance factor of the WT and the mutants. IC_{50} (=inhibitory concentration) is the concentration needed to inactivate 50 % of the PS II.

The figure 3.5(a) shows the inactivation of PS II by DCMU in the WT and in SA-264. In comparison to the WT the inactivation is delayed in the mutant. At a concentration of $1 \cdot 10^{-5}$ M (all PS II are still active in the mutant) about 60 % of the PS II reaction centers of the WT are already inactivated by the herbicide. By comparing the concentration which is needed to inactivate 50 % of PS II (IC_{50}) the resistance factor can be calculated. The list in the table (Fig 3.5(b)) shows the IC_{50} and the resistance factor of the mutants compared to the WT. The resistance factor is 3 for VI-219, 150 for FI-255, 3000 for SA-264 and 500 for LW-275.

The resistance of the mutants to DCMU is due to a change in the structure of the Q_B binding niche in a way that impairs the binding capacity of DCMU (but also of Q_B).

3.3.2 Fluorescence Induction Kinetics

In order to compare the effect of the different mutations on the electron transport, fluorescence induction kinetics (also called the 'Kautsky effect') were analysed. This effect represents the variation of the Chl *a* fluorescence emission as a function of time under exposure to continuous light (Krause and Weis, 1991). The shape of the fluorescence induction kinetic is depending upon the redox state of the electron transport chain between the PS II and PS I and is characteristic for different taxonomic groups (Parésys *et al*., 2005). The kinetics were recorded for red light only at different light intensities. In Fig 3.6(a) the WT and LW-275 kinetics are shown for different light intensities as an example for the fluorescence induction kinetics. The extent of the rise of F_0 to F_i is equivalent to the extent of Q_A reduction. F_i rises with increasing light intensity, because under high light conditions more photons are available for PS II reaction centres. Cells under high light are therefore able to catch more photons and have more energy for reducing Q_A. The figure also shows the difference between the mutant and the WT: the rise to F_i with increasing light is higher in the mutant in comparison to the WT. The higher extent of F_0 to F_i is due to the mutation which is impairing the reoxidation of Q_A (the electron transfer between Q_A and Q_B) so that the time Q_A remains reduced is longer, generating this higher fluorescence level in LW-275.

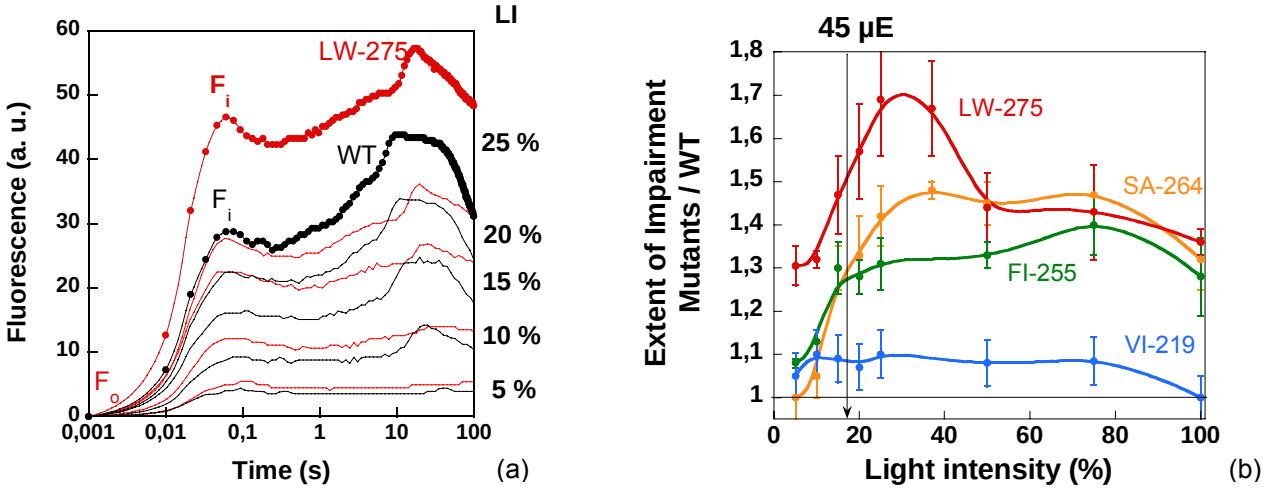

***Fig.* 3.6: Fluorescence Induction Kinetics of the WT and the Mutants.** **(a)** Example for recorded sequence of WT and LW-175 for different light intensities (LI). **(b)** Evaluation of the extent of impairment of electron transport rate for the mutants compared to WT.

The ratio F_i(mutant)/F_i(WT) can then be used to evaluate the impairment of the electron transport rate (Fig 3.6(b)).
At the standard light intensity used to culture the diatoms (45 $\mu E \cdot m^{-2} \cdot s^{-1}$) VI-219 shows only minimal impairment of a factor of 1.08 compared to the WT while FI-255 and SA-264 are impaired by a factor of 1.27 and 1.3 respectively. The highest inhibition of electron transport is observed in LW-275 with a factor of 1.5. This means that, due to the mutation in LW-275 only 2 electrons are transferred from Q_A to Q_B while WT is transporting 3 e^- at the same time.

3.4 Architecture of the Photosystems

To see whether the mutations and the resulting impairment in electron transport have an effect on the architecture of the photosystems, the amount of active PS II and the antenna size were measured.

3.4.1 Number of PS II

For estimating the amount of active PS II, the oxygen evolution was measured with the rate electrode. Here the relative O_2 yield produced per flash during a sequence of single-turnover saturating flashes is recorded. The steady-state O_2 yield per flash (Y_{SS}) is attained for the last flashes of a sequence of 20 flashes when the classical four-step oscillations due to the S-states cycle (Kok *et al*., 1970) are fully damped. Y_{SS} was used to evaluate PS II activity since it reflects the relative concentration of oxygen evolving (active) PS II reaction centers.

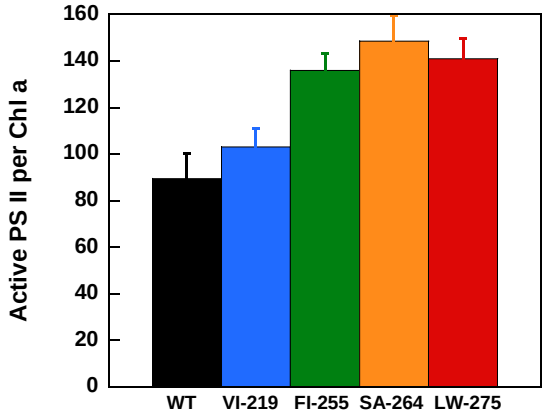

***Fig 3.7*: Amount of active PS II per Chl *a* in WT and the Mutants.** Plot resulting from the measurements with the rate electrode, showing the amount of active (oxygen evolving) PS II in WT and the mutants.

As shown in figure 3.7, VI-219 has about 1.15 x more active PS II, FI-255 1.52 x more, SA-264 1.66 x and LW-275 1.57 x more oxygen evolving PS II in comparison to the WT.

To verify the data, Western Blot experiments were performed. Protein was extracted as described in 2.4.9 and loaded on a SDS gel (see 2.4.10). In order to check, whether an increase of a factor of 1.5 can actually be detected by the Western blot method, different amounts of WT protein were loaded on a gel and subsequently the Western Blot was performed. As can be seen in figure 3.8(a) the differences between the various amounts of protein can be clearly seen. For the blot with the different mutants the amount of protein equivalent to 1 µg Chl *a* was loaded on the SDS gel (see 2.4.10) The samples were normalized to the same amount of Chl *a* to simplify comparison with the results from the rate electrode measurements. After blotting the proteins on a PVDF membrane, it was subsequently blocked and incubated with an antibody against the protein D1.

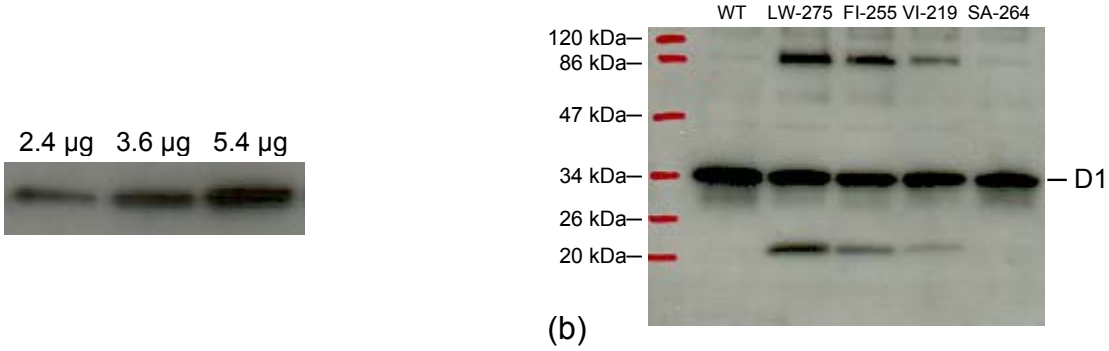

***Fig. 3.8*: Western Blot against D1. (a)** Western Blot performed with different amounts of WT protein. (b) Western Blot with protein equivalent 1 µg Chl *a*.

As shown in figure 3.8(b) a strong signal was detected, but verification of the previous result failed. No significant increase of D1(32 kDa) in FI-255, LW-275 or SA-264 can be seen. Instead, in LT-275, FI-255 and VI-219 other signals are seen at about 20 kDa and 86 kDa.

3.4.2 Antenna Size

By measuring the steady state oxygen yield with the rate electrode with different flash intensities, the size of the antenna of the PS II reaction centre was estimated. Different combinations of neutral filters were used to decrease the intensity of the incoming flashes. The obtained values for Y_{SS} were then plotted against the

corresponding flash intensity (Fig. 3.9). By comparing the different flash intensities which are required for reaching 50 % of the steady state oxygen yield, estimations about the different antenna sizes can be made. For example, if there's more energy (higher flash intensity) required for the mutant to reach the same level of oxygen yield, then the antenna size of the mutant is smaller, as it needs more photons to reach the same level of oxygen emission. The WT on the other hand has a bigger antenna and therefore can catch more photons at the same intensity or, in other words, needs less energy to reach the same level of oxygen yield.

The flash intensity required to reach 50 % of the Y_{SS} is the same for the WT and VI-219, indicating that those two strains have the same antenna size. In contrast, the other mutants need more energy (higher light intensity) to reach this oxygen level, which is an indicator, that their antenna size is smaller. When illuminated with the light intensity sufficient for the WT and VI-219 to reach 50 % of the steady-state oxygen yield, the other mutants (FI-255, SA-264 and LW-275) cannot catch the same amount of photons because of the smaller antenna. They are not able to catch the same amount of energy and therefore cannot reach the same oxygen yield.

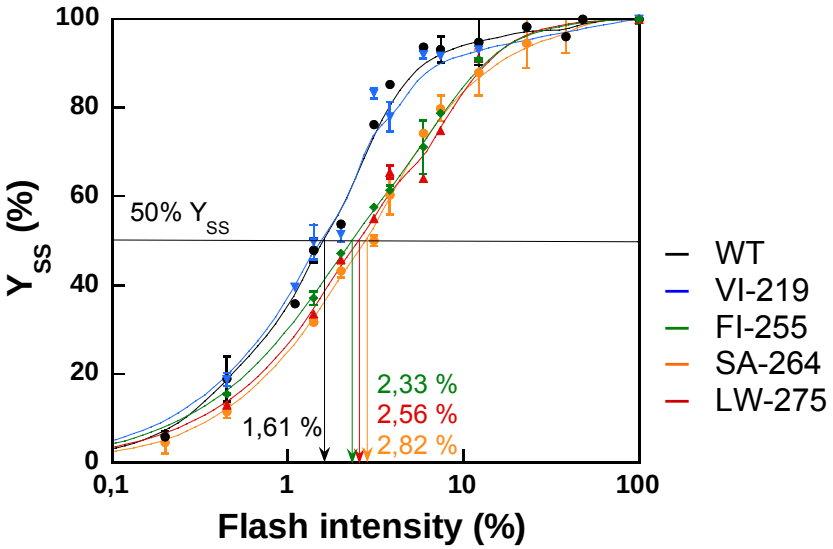

***Fig 3.9*: The steady-state Oxygen Yield (Y_{SS}) for WT and the Mutants depending on the Flash Intensity.**

The antenna size is smaller in FI-255 by a factor of 1.45, in LT-275 by a factor of 1.59 and in SA-264 by a factor of 1.75.

3.5 Oxygen Measurements

3.5.1 Oxygen Measurements with the Clark Electrode

To investigate the effect of the mutations on photosynthesis, measurements with the Clark Electrode were performed. In contrast to the rate electrode the global oxygen production is measured here. The cells are incubated in a vial which is illuminated with continuous light provided by a lamp. The emitted oxygen is recorded as a function of time. During incubation of the cells in the dark, a decrease of oxygen can be observed which is due to respiration of the cells. When switching on the light the cells are using this energy to oxidize water at the oxygen evolving complex where O_2 is finally liberated. An increase of oxygen can be measured.

In this experiment the cells were illuminated for 5 min with different light intensities after adaptation to darkness for 15 min (Fig. 3.10). Recording was started after 10 min of dark-adaptation, observing the 'initial' respiration in the dark which should be the same for all light intensities. During illumination of the cells oxygen production can be measured, which is the net photosynthesis (oxygen that is released to the medium). After illuminating the cells, the oxygen evolution was recorded for another 5 min in the dark in order to get the 'final' respiration. Gross photosynthesis was then calculated as net photosynthesis – 'final' respiration.

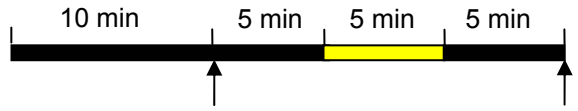

***Fig. 3.10*: Scheme of Illumination of the Cells.** Start and end of recording are indicated by arrows.

The gross oxygen production was then plotted against the corresponding light intensity to get the so-called P–E curves (photosynthesis – irradiance) (Fig. 3.11).

Two parameters are obtained from the curves: the maximal global photosynthesis (P_{max}) and the light intensity for which this maximal level is reached which is equivalent, with the saturating light intensity.

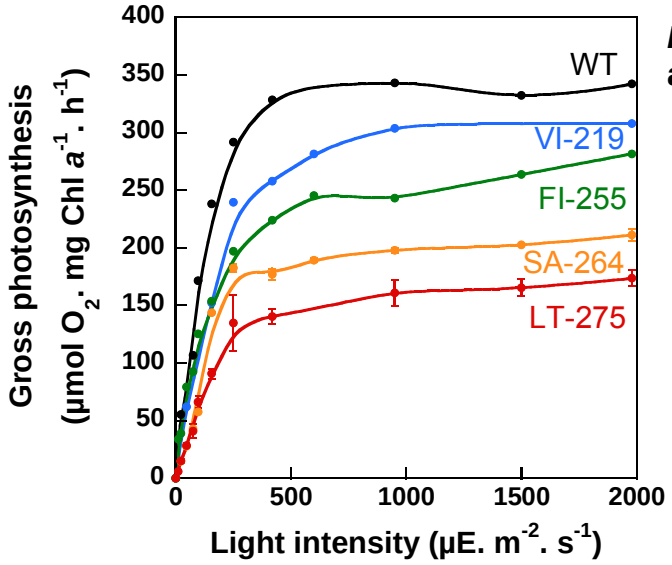

***Fig. 3.11*: P–E Curves of the WT and the Mutants.**

Gross photosynthesis is highest for WT followed by VI-219, FI-255, SA-264 and LW-275. The maximal global photosynthetic level is reached at a light intensity of 600 µE (=µmol photons)·m^{-2}·s^{-1} for WT, VI-219 and FI-255. For SA-264 and LW-275 this level is already reached at 300 µE·m^{-2}·s^{-1}.

3.5.2 Photoinhibition Kinetics

The amount of active PS II was measured after illumination of the cells to see the oxygen evolution of the mutants in the light. Two different measurements were done. First, the cells were illuminated for 5 min under various light intensities in the reaction chamber of the Clark Electrode before measuring the amount of active PS II with the rate electrode. Second, the cells were illuminated with oversaturating light (2000 µmol photons·m^{-2}·s^{-1} which is corresponding to full sunlight in nature) for 2.5, 5, 15, 30 and 45 min prior to measurements with the rate electrode. These measurements were not done for LW-275 because it was impossible to calculate a steady-state oxygen yield, since the PS II cycle was too high (see 3.7.2).

As above, the amount of active PS II in % was plotted against the light intensity (Fig. 3.12).

In the first experiment (Fig. 3.12(a)), VI-219 and FI-255 show no significant difference in comparison to the WT, while the amount of active PS II is decreasing very rapidly in SA-264 compared to the WT. For example, at a light intensity of 400 µE·m^{-2}·s^{-1}, when 95 % of WT PS II are active, only 84 % of the PS II in SA-264 are still active.

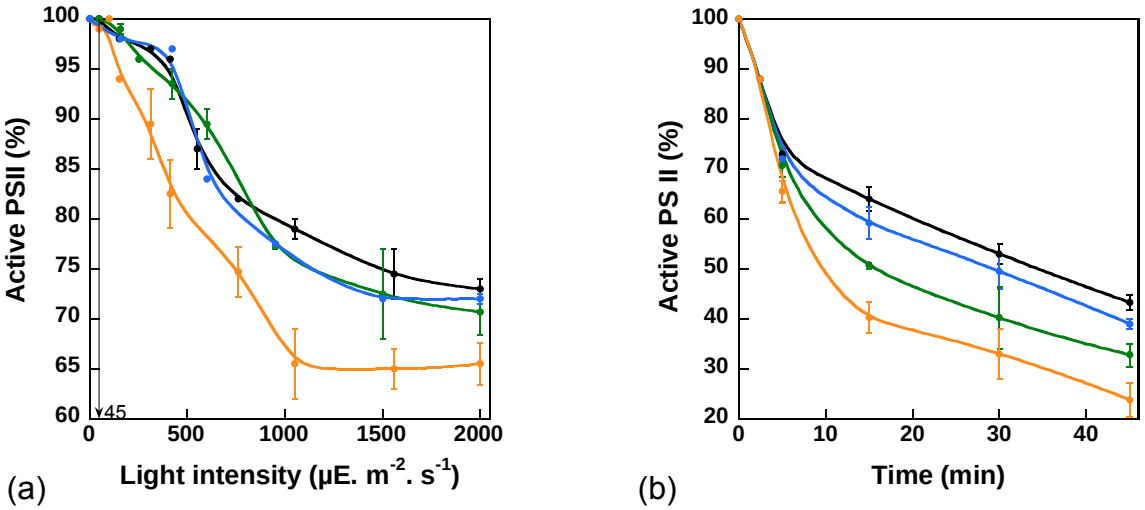

Fig. 3.12: **Photoinhibition Kinetics of the WT and Mutants. (a)** Amount of active PS II after illumination of the cells for 5 min. **(b)** Amount of active PS II after illumination at 2000 µmol photons·m^{-2}·s^{-1} for different times.

When exposed to oversaturating light for different periods of time (Fig. 3.12(b)), VI-219 shows only a slight decrease of active PS II in comparison to WT, while FI-255 has already 20 % less active PS II after 15 min of illumination. This factor of decrease is stable for longer illuminations. SA-264 shows a very strong decrease in PS II activity, having 40 % less active PS II after 15 min of illumination compared to WT. 50 % of active PS II is reached after 34 min in WT, in VI-219 after 30 min, in FI-255 after 16 min and in SA-264 already after 10 min. It is also obvious, that in all cases the highest decrease is observed during the first 15 min, after that the decrease of active PS II seems to be linear with the time.

3.6 High Light

As sensitivity to high light was observed during the Photoinhibition Kinetics, investigations on growth of the cells under high light were performed. For these experiments the light intensity was adjusted, that it was just saturating for the WT. Like for the growth curves under low light, samples of the cells were taken daily and used for measuring the amount of Chl *a*. The concentration of Chl *a* was then plotted against the time (Fig. 3.13).

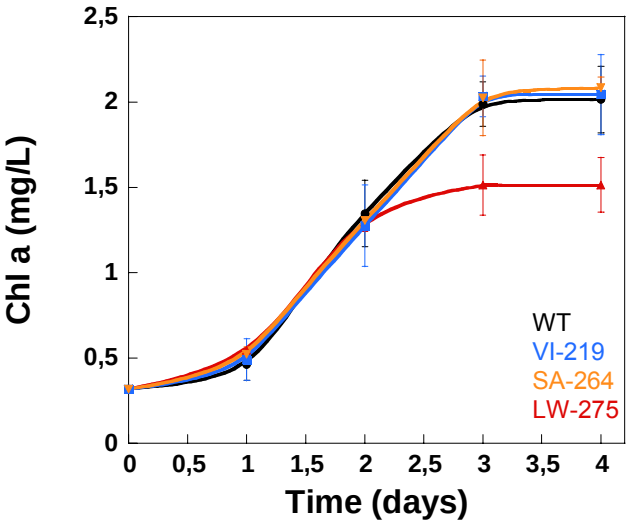

***Fig. 3.13*: Growth Curves of the WT and the Mutants under high Light (400 µmol photons·m^{-2}·s^{-1}).**

All cultures grew slower as compared to low light conditions. In addition they also had a lower final Chl *a* concentration (25 %) compared to WT under low light conditions. Under high light WT, VI-219 and SA-264 had an exponential phase of two days and a growth rate of 2.6 x·day^{-1}. LW-275 grew like the WT for the first two days, but reached its stationary phase already on day 3. Growth of FI-255 was not evaluated since growth was varying too much.

3.7 Photoprotection

It is known that diatoms have developed different strategies to protect themselves from over-excitation. The main protective mechanisms appear to be non-photochemical quenching of the chlorophyll excited state (NPQ) (Ting and Owens, 1993) and a cyclic electron flow around PS II (Lavaud *et al*., 2002).
Analysis of NPQ and the PS II electron transfer cycle were performed in WT and the mutants.

3.7.1 NPQ

NPQ was measured using a pulse amplitude modulated (PAM) fluorometer as described in 2.5.1.2. As this instrument is usually used for leaves of plants and not for algal suspensions, cells equivalent to 10 µg Chl *a* were concentrated to on a Millipore glass fibre prefilter which was then placed in the measuring area of the PAM.

After measuring F_0 and F_m with the measuring light and a saturating flash (as described in 2.5.1.2), the cells were illuminated with different intensities of actinic light varying from 1 to 1207 µE (µmol photons)·m^{-2}·s^{-1} to measure F_m'. With the formula given in 2.5.1.2 the values for NPQ were calculated and plotted against the corresponding light intensity (Fig. 3.14).

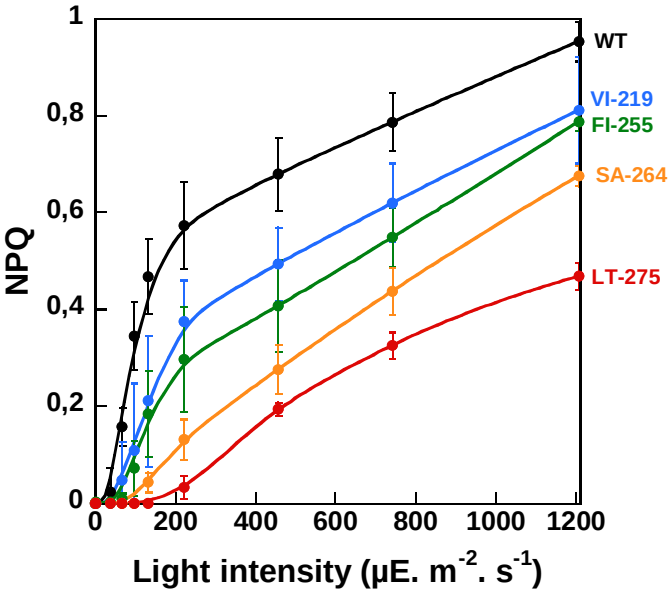

***Fig. 3.14*: NPQ of the WT and the mutants for different light intensities.**

WT showed the highest values of NPQ followed by VI-219 and FI-255. SA-264 revealed 40 % and LW-275 14 % of the NPQ of the WT at a light intensity of 200 µE·m^{-2}·s^{-1} and higher.

3.7.2 PS II Cycle

For estimating the oxygen deficit (indicator for the PS II cycle) with the rate electrode, the cells were illuminated for 5 min with various intensities in the reaction chamber of the Clark Electrode prior to measurement. The oxygen deficit was quantified with the formula given in 2.5.2.2 and plotted against the corresponding light intensity (Fig. 3.15).

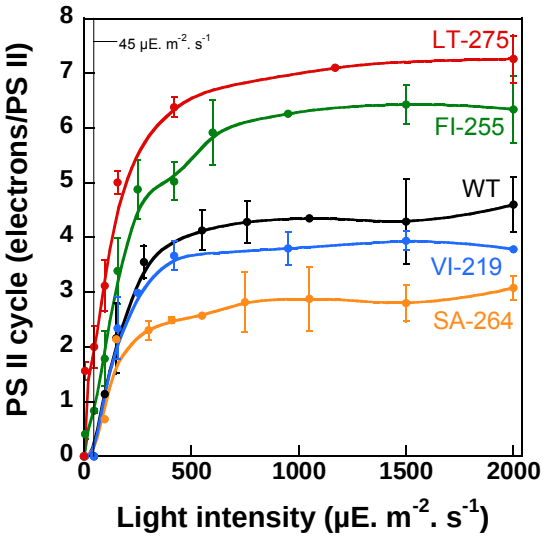

***Fig. 3.15*: PS II Cycle of the WT and the Mutants.** Light Intensity under which the cells were grown is indicated by a vertical line.

Oxygen deficit is the highest in LW-275 with a maximum of 7 e^- cycling around PS II. In FI-255 maximally 6 e^- cycle around PS II (1.5 x of the maximum PS II cycle of the WT (about 4 e^-/PS II)). The oxygen deficit is similar in VI-219 and about 70 % of the WT in SA-264 (3 e^-/PS II). At the light intensity used to culture the cells already 2 electrons are cycling around PS II in LW-275 and about 1 electron in FI-255, while in the WT and the other mutants no oxygen deficit is observed.

3.8 Preparations for Gene Expression Analysis

3.8.1 Synthesis of DIG-labeled Probes

For synthesizing the digoxigenin-labeled probes, primers had to be designed first. Upstream and downstream primers were about 20 to 25 basepairs (bp) long. They were selected in a way, surrounding a region within the target gene of a length of 400 to 500 bp. To permit strong binding, the 5' end of each primer was rich in GC content. The annealing temperature was chosen around 58 °C. Five different probes were synthesized, binding in high-light induced protein A (hliA), high-light induced protein B (hliB), fucoxanthin chlorophyll protein (fcpA), diadinoxanthin de-epoxidase (DDE) and 18 SrRNA.

A test-PCR was performed using *Taq*-polymerase and a variety of annealing temperatures ranging from 50 to 61 °C. After analysis by horizontal gel electrophoresis, the annealing temperature resulting in the purest product was selected for synthesis of the probes. When analyzing the probes with gel electrophoresis, it is crucial that the fragments appear to be larger as expected,

which is due to the added digoxigenin labels. For example the fragment hliB (484 bp) appears as a band of about 750 bp. hliA (610 bp) appears at about 900 bp, fcpA (541 bp) at 800 bp, DDE (584 bp) at 800 bp and finally 18SrRNA (580 bp) at 800 bp (Fig. 3.16).

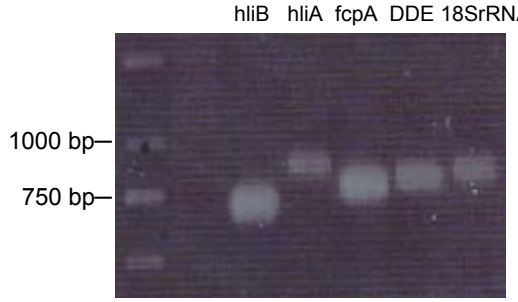

***Fig. 3.16*: Purified Probes analyzed with horizontal Gel Electrophoresis.**

Synthesis and purification of the DIG-labeled probes was performed as described in 2.4.15. To estimate the concentration of the probes the dot blot method was used. Here, a control with a known concentration of DNA and the samples of unknown concentrations are diluted in various steps and blotted on a membrane (for details see 2.4.16). An estimation of the concentration of the probes can be made by comparing the intensity of the dye of the probes with the control (Fig. 3.17).

The first sample which can be seen with the control is DNA (1 ng·µL^{-1}) followed by a sample of 0.1 ng·µL^{-1} and finally of 0.01 ng·µL^{-1}.

(a)

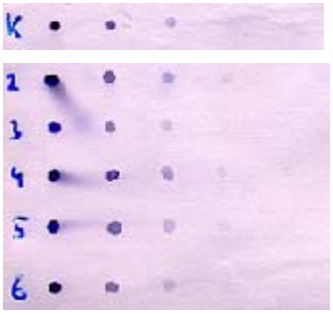

(b)

Probes	Estimated concentration
hliB	50 ng/µL
hliA	20 ng/µL
fcpA	70 ng/µL
DDE	50 ng/µL
18SrRNA	20 ng/µL

***Fig. 3.17*: (a) Dot Blot of the Control and the Probes.** K: control, 2: hliB, 3: hliA, 4: fcpA, 5: DDE, 6: 18SrRNA. **(b) Table giving the estimated Concentrations of the Probes.**

For the probes binding in hliB (2) and DDE (5) a concentration of about 50 ng/µL each was estimated, while the probes binding in hliA (3) and 18SrRNA (6) have a concentration of about 20 ng/µL. The probe binding in fcpA (4) has the highest estimated concentration of about 70 ng/µL.

3.8.2 Test of the Probes via Northern Blot

To check the binding capacity of the probes, they were tested in Northern Blot experiments. For this, RNA was extracted from cells growing in the dark for 24 h and for cell growing under low light. The protocol for RNA extraction is described in 2.4.13. Separation was performed by denaturing horizontal gel electrophoresis. The protocol used to perform the Northern Blot is described in 2.4.17.

In figure 3.18 preliminary results are shown for the Northern Blot performed with the probe binding in 18SrRNA.

A strong signal was detected for the dark-adapted and the low light cells. This indicates that the probe is binding correctly. The presence of various unspecific bands demonstrated that the hybridization conditions have to be optimised.

***Fig. 3.18*: Northern Blot using the Probe binding in 18SrRNA.** On the left side RNA from dark-adapted cells was loaded, on the right side RNA from cells in the light.

3.9 Screening for further Integrations of mutated D1 in the Chloroplast Genome

As it was still unclear how the mutants actually were obtained Southern Blot experiments were performed to exclude the possibility of episomal integration of mutated *psbA* (coding for DI) genes that might allow spontaneous mutations in the chloroplast genome. The Southern Blot was performed as described in 2.4.12. As a control, *Sca*I digested WT DNA was mixed with two different transformation vectors $D1_{3.5}$ (3.5 kb long) and $D1_2$ (2 kb long). As shown in figure 3.19 two different bands can be detected with the controls while in the WT and the mutants only 1 band is visible indicating, that there are no episomes or any further integrations of *psb*A.

As can be seen from the blot the probe seems to bind correctly, although various unspecific bands appear which could result from unspecific binding of the probe or overloading of the gel.

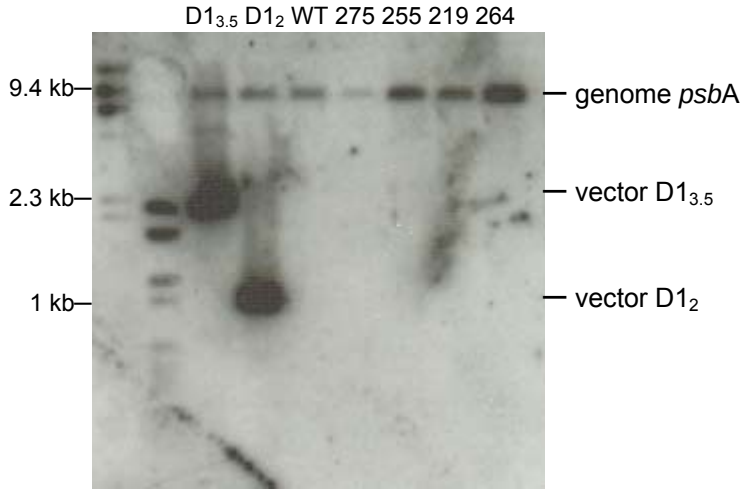

***Fig. 3.19*: Southern Blot performed with a Probe against *psb*A.** D1$_{3.5}$ is the control containing a 3.5 kb vector; D1$_2$ is the control containing a 2 kb vector. 275: LT-275 mutant, 255: FI-255, 219: VI-219, 264: SA-264.

4 Discussion

4.1 Influence of the Mutations on the Electron Transport within PS II

After localizing the mutations within the *psb*A gene (see 3.1) different measurement were performed to investigate the influence of the mutations on binding of Q_B and DCMU (as the mutation changes the binding capacity of DCMU) to the D1 protein of the Photosystem II reaction centre (PS II_{RC}). Binding of Q_B was measured indirectly through the redox state of Q_A.

The mutation at position 219 (V→I) is located in the transmembrane α-helix D, which is not close to the Q_B binding pocket. It therefore does not have a great influence on the binding of Q_B or DCMU in the niche, which can be seen from the low resistance to DCMU as well as from the weak effects on the electron transport (the binding of Q_B is hardly inhibited). This is different to the mutation at position 255, which is close to the Q_B binding pocket and therefore has more influence on the binding of Q_B and DCMU. Here, resistance to the herbicide as well as the impairment in electron transport is stronger. These effects are even more visible in the SA-264 mutant. Its mutation lies within the Q_B pocket and is assumed to be directly involved in the binding of Q_B (Xiong *et al*., 1996). It is supposed to provide hydrogen bonds to the carbonyl oxygen atoms of Q_B and appears to coordinate the binding to the herbicide DCMU. This would explain on one side the high resistance to DCMU; on the other side the binding capacity of Q_B is also influenced by this amino acid change and therefore the electron transport is impaired. The amino acid change from Leucine to Tryptophan at position 275 is located in the transmembrane α-helix E. Although it is not located within the Q_B pocket, it has a strong influence on the electron transport from Q_A to Q_B. The mutation is located near a histidine (position 272) responsible for binding of a non-heme iron. This iron atom is supposed to be involved in the maintenance of structure and function of the Q_A and Q_B binding niches and therefore affects the transport of electrons within the PS II reaction centre. Further the mutated residue is at the interface of D1 and D2 and considered to be involved in the correct assembly of the PS II (Vermaas *et al*., 1994). That would explain the high impairment in electron transport but the relative low resistance to DCMU. The mutation does not

reduce the binding capacity of Q_B, but inhibits the transfer of electrons coming from the Q_A to it.

Mutations at the same positions of the D1 protein were already described in *Chlamydomonas reinhardtii* (Erickson *et al*., 1989). Erickson and co-workers studied the resistance to different herbicides as well as the rates of electron transfer between Q_A and Q_B. They found the highest resistance to DCMU in SA-264 and VI-219 with a factor of 20 and the lowest resistance in the strain mutated at position 255 with a factor of 0.5. The mutant altered at position 275 had a resistance factor of 5. In contrast, in this study the highest resistance to DCMU was measured in SA 264 while almost no resistance was found in VI-219. Besides the differences in DCMU resistance, Erickson *et al*. also found different factors for inhibition of the electron transport. They observed no impairment in electron transport in all mutants except SA-264, while in this study all mutants except VI-219 were affected in the electron transport. The influence of the different mutations on the binding at the Q_B binding niche seems to be different in diatoms and green algae. It suggests a somehow different structure of the PS II reaction centres which might be due to the different origins of the plastids. Noteworthy, several authors already pointed out the similarity in PS structure shared by diatoms and cyanobacteria (Martinson *et al*., 1998).

4.2 Changed Architecture of the Photosystems in the Mutants

The amount of active (oxygen evolving) PS II is increased in the mutants (3.4.1) and this increase appears to be proportional to the impairment in electron transport. There also seems to be a maximal factor of increase in the amount of PS II. Although the LW-275 mutant is much more impaired in the electron transport in comparison to the SA-264 mutant, it has the same amount of active PS II. The increase factor of 1.6-1.7 which was measured for SA-264 and LW-275 seems to be the maximum factor for increasing the amount of PS II. With a higher amount of oxygen evolving PS II all mutants, except LW-275 are able to compensate the impairment in electron transport in low light. This is obvious from the growth rates, which are the same for the mutants and WT. This is especially true for FI-255 and SA-264, which are impaired by a factor of about 1.3 but reach the same final biomass level. The compensatory effect is also visible from the values for the maximal photosynthetic capacity F_v/F_m. For the mutants values around 0.7 are obtained for cells in the

exponential growth phase. At the same time this value is also found in the WT and is the general value for diatoms in this phase of growth (Paresys *et al*., 2005). In LW-275 a different situation is observed. Although an increase of active PS II by a factor of 1.6 was measured, it is apparently not sufficient to compensate the impairment in electron transport. This is the reason why LW-275 has a lower growth rate than the WT or the other mutants and might explain the lower F_v/F_m value of 0.57.

It was not possible to evaluate the increase in PS II within the mutants with the Western Blot. The system was developed successfully and proven to be sensitive enough to detect different amounts of D1. However, it was not clear whether the differences in D1 content within the protein loaded on the SDS gel represent the varying D1 contents in the mutants. This is due to the fact that the normalization (to the same amount of Chl *a* per volume of culture) takes place before protein extraction and the extractions themselves may differ in their effectivities. When looking at the blot shown in 3.4.1 it seems that the signal is oversaturated, preventing clear recognition of signal differences. It is possible that not all of the extracted protein was resolved which even increases the failure. This experiment has to be repeated under optimized conditions for the protein extraction to verify the data coming from the measurements with the rate electrode. Ohad *et al*. (1990) constructed two different mutants which were altered at the position 264 and 255 in the D1 protein. By immunoblotting they found a slight increase in D1 in the mutants compared to WT but no correlation with the also observed impairment in electron transport is mentioned. In this study it is proposed that the increase in PS II is a ‘compensatory mechanism’ for the impairment in electron transport.

On the Western Blot two other bands occurred in the mutants VI-219, FI-255 and LW-275. In contrast to D1 (32kDa) they had the size of approximately 86 kDa and 21 kDa. In higher plants such bands are usually detected when the cells are exposed to light stress and correspond to degradation products of D1 (Barbato *et al*., 1995). The D1 protein rapidly turns over within the thylakoid membrane (reviewed by Edelmann *et al*., 1984). This process of degradation and synthesis is light-dependent and thought to be a repair mechanism to replace D1 subunits within PS II complexes that have been damaged by excess light (Barber and Andersson, 1992). Ohad *et al*. (1990) demonstrate a close link between Q_B^- (semireduced quinone) destabilization in PS II and the mechanism controlling the light-dependent turnover of D1 in *Synechococcus*. They suggest that destabilization of the semireduced quinone (due

to mutation of the Q_B pocket), facilitates a light-induced damage in D1 which triggers its degradation and therefore increases the turnover of D1. This was not investigated in further experiments here, but the observed fragments on the Western Blot could be a hint, that the process lying behind the degradation of D1 is similar in diatoms and cyanobacteria.

Decrease of the antenna size per PS II was measured. Again, proportionality with the amount of active PS II can be observed. The mutant which has the highest amount of active PS II also has the smallest antenna per PS II (SA-264), while WT and VI-219 who have less PS II than the other mutants have the largest antenna, so that the total antenna surface per chloroplast is the same in all strains. The decrease of the PS II antenna size could be a secondary effect, if the cells are not enlarging the overall antenna surface per chloroplast. This means that the antenna is differently distributed amongst the PS II reaction centres and when more PS II_{RC} are present, the antenna size per PS II decreases. Lack of change in the global antenna size surface (and consequently in PS II antenna size) can be seen as a way to reduce the excitation pressure on PS II. On the other hand, it could result from a disturbance in the regulation of *fcp* genes through the plastoquinone redox state due to mutations (to be checked with gene expression analysis).

To see whether the increase of the amount of PS II is concomitant with an increase in PS I, the amount of PS I per PS II was measured by Johann Lavaud at the ENS Paris using a 77 K fluorescence emission spectra at 440 nm (absorption peak of Chl *a* in the blue region of the visible spectrum of light) from 600 to 800 nm with a spectrofluorometer (F-4500 Hitachi). In figure 4.1(a) an example for the emission spectra for the WT, SA-264 and LW-275 is shown. The different spectra were normalized to the same fluorescence level of PS II. As can be seen in the figure, the fluorescence level at 711 nm is higher in LW-275 which is due to the higher amount of PS I versus PS II in the mutant.

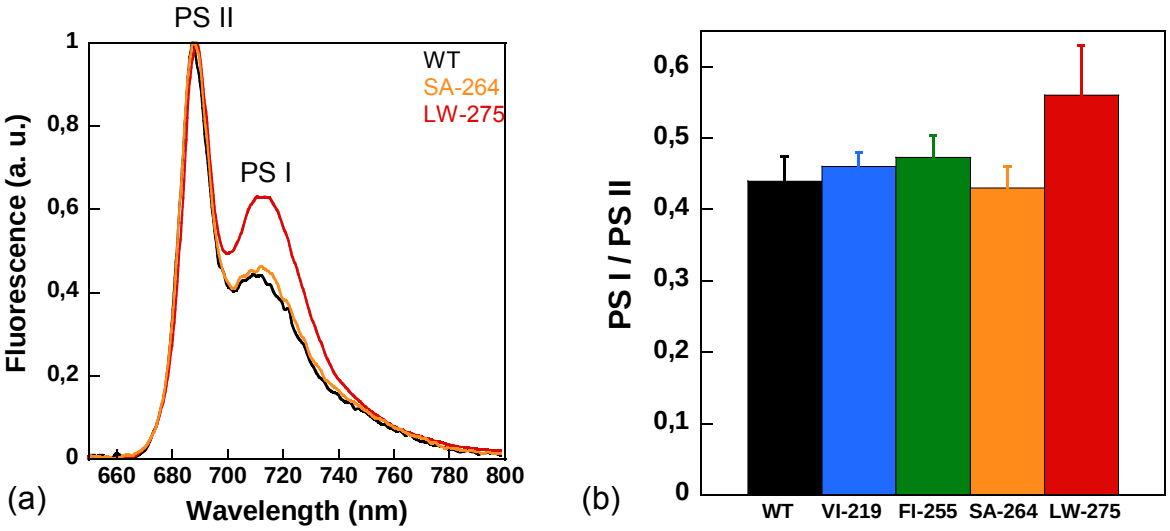

***Fig 4.1*: Ratio of PS I/PS II in the WT and the Mutants. (a)** Example for the emission spectra of the WT, SA-264 and LW-275 obtained from the measurements using a 77 K fluorescence emission spectra at 440 nm with a spectrofluorometer. **(b)** Amount of PS I per PS II in the WT and the mutants, calculated from the fluorescence difference at 711 nm after normalization to the same fluorescence level of PS II.

As shown in Fig. 4.1(b) all mutants except LW-275 have about the same PS I/PS II stochiometry. LW-275 has 1.2 times more PS I than the WT. This is probably a reaction to the fact, that the increase in the amount of PS II is not sufficient to compensate the impairment in electron transport in LW-275 (see above).

A comparative example of how the organization and structure of the PS II reaction centres in the WT and the mutant LW-275 could look like is shown in Fig. 4.2.

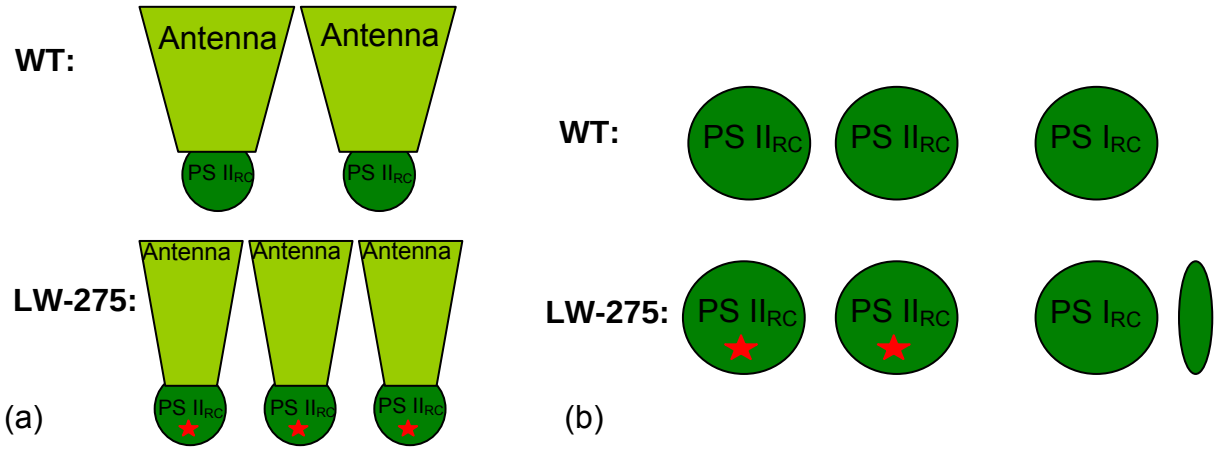

***Fig 4.2*: Comparison of the Organization and the Structure of PS II in the WT and the Mutant LW-275. (a)** Amount of PS II and Antenna size in WT compared to LW-275. **(b)** Amount of PS I reaction centers (RC) per PS II reaction centers in WT and LW-275. The mutation in the PS II reaction center of the mutant is indicated by a red star.

The mutant has more active PS II reaction centers (RC) per Chl than the WT, at the same time the antenna of those RC is smaller in LW-275. Also, this mutant has more PS I_{RC} per PS II_{RC}. A similar organisation is predicted for SA-264 and FI-255 except the increase in PS I. For VI-219, only the PS II amount is slightly increased.

4.3 Consequences of the Mutations on the Photosynthetic Activity

As described in 3.5.1 two parameters can be seen from the P–E curves. Besides the maximal photosynthesis (P_{max}), the light intensity (saturating light intensity) needed to reach this oxygen level can be defined. For WT, VI-219 and FI-255 the maximal level is reached at a light intensity of 500 $\mu E \cdot m^{-2} \cdot s^{-1}$ while an intensity of 300 $\mu E \cdot m^{-2} \cdot s^{-1}$ is already enough in SA-264 and LW-275. It is unlikely that this is due to the impairment in electron transport, as for example FI-255 which is impaired by the same factor as SA-264 does need as much energy (500 $\mu E \cdot m^{-2} \cdot s^{-1}$) as the WT to reach the maximal photosynthesis level. Moreover it is assumed that the cells increase their amount of PS II to compensate the effect of the impairment (4.2). If the difference in saturating light intensities would come from the impaired electron transport, the mutants except LW-275 should behave like the WT due to the increase in the amount of PS II. This is not true for LW-275, since it is impaired by a higher factor compared to SA-264 but has the same amount of PS II.

An explanation can be found by looking at the photoinhibition kinetics (3.5.2). In the first part of the experiment the oxygen evolution was measured for cells that were illuminated for 5 min under varying light intensities. A look at the light intensities at which the saturating oxygen level is reached in the P–E curves, reveals, that at this point approximately 90 % of the PS II are still active. For SA-264 for example the amount of active PS II is decreasing very fast with increasing light. At a light intensity of 300 $\mu E \cdot m^{-2} \cdot s^{-1}$ as already said about 90 % of the PS II are still active, while at a light intensity of 500 $\mu E \cdot m^{-2} \cdot s^{-1}$ (saturating light intensity for WT) only 80 % are active. It seems that with the light intensity needed to reach 90 % of active PS II, the level of maximal gross photosynthesis is reached.

In addition to the varying saturating light intensities, different final oxygen levels of the P–E curves are observed. WT has the highest level (Fig. 3.10) with about 350 µmol $O_2 \cdot$mg Chl $a^{-1} \cdot h^{-1}$ and LT the lowest level with about 150 $O_2 \cdot$mg Chl $a^{-1} \cdot h^{-1}$. This

is partially due to the lower light intensity needed to reach the saturating level and partially due to the sensitivity to high light (4.3).

4.4 Photoprotection

As shown in chapter 3.7 different photoprotective mechanisms such as NPQ (non-photochemical quenching) and the PS II cycle were measured. NPQ is supposed to dissipate excess excitation energy through a harmless non-radiative pathway. The partitioning of absorbed energy between transfer to the reaction centre and photoprotective non-radiative dissipation is controlled by the trans-thylakoid pH gradient (reviewed by Müller *et al*., 2001) and by the reversible conversion of epoxidized to de-epoxidized forms of xanthophylls (the so-called xanthophyll cycle) (Gilmore, 1997). The molecular mechanisms of photoprotection have mostly been studied in higher plants (Demmig-Adams and Adams, 1996). Several mutants of Arabidopsis and *Chlamydomonas reinhardtii* with modified violaxanthin content and NPQ extent have been investigated (Müller *et al*., 2001). Also, a violaxanthin independent, ΔpH dependent NPQ can be observed in higher plants (Gilmore and Yamamoto, 1991).

In diatoms non-photochemical quenching is dependent on the formation of a transthylakoid proton gradient (ΔpH) and on de-epoxidation of diadinoxanthin (DD) to diatoxanthin (DT) (Lavaud et al., 2002d). The diadinoxanthin-deepoxidase (DDE) catalyzes the latter reaction and is activated by changes in ΔpH under excess light (Jakob and Wilhelm, 2001). The de-epoxidation of diadinoxanthin to diatoxanthin increases NPQ and thus protects the PS II from over-excitation. This reaction is fully reversible in the dark; DT is epoxidized by an epoxidase forming DD.

As the mutants are inhibited in linear electron transport they cannot reach the same ΔpH as WT, therefore non-photochemical quenching is lower which results in stronger sensitivity to high light. The compensatory mechanism (increase in PS II) described before is enough to compensate the impaired electron transport under low light, but is obviously not sufficient to ensure an electron transport rate high enough under high light. This would explain the different NPQ values which are proportional to the impairment in electron transport. Measurements for VI-219 and FI-255 should be repeated, as the standard deviations are quite high, but nevertheless the

tendency seems to be as expected, with VI-219 having higher NPQ-values than FI-255.

Another mechanism that protects the cells from photo-oxidative damage is the so-called PS II electron cycle (Lavaud *et al*., 2002b). As already mentioned in 1.3.2 this has already been suggested earlier as a protective mechanism (Barber and De Las Rivas, 1993) and was shown to occur *in vivo* in the green alga *Chlorella pyrenoidosa* at high light intensities (Falkowski and Kolber, 1986).

As shown in figure 3.14 cyclic electron flow is the highest in LW-275 and the lowest in SA-264. Under growth conditions (45 $\mu E \cdot m^{-2} \cdot s^{-1}$), LW-275 already showed a cycling of 2 electrons around PS II, indicating that this irradiance is already high for this mutant. Obviously the impairment in electron transport is so high, that even at 45 $\mu E \cdot m^{-2} \cdot s^{-1}$ the cells are stressed as illustrated by the lower F_v/F_m. The increase of the PS II electron cycle in LW-275 and FI-255 allows the cells to reduce the probability of over-reduction in the PS II. This is believed to be a direct response to the impairment of the electron transport rate. It seems that a value of 6-7 electrons/PS II is a maximal threshold. In SA-264 the cycle around PS II is lower than in WT unless, the same pattern a LW-275 and FI-255 should be expected. This might be due to the mutation itself which probably disturbs the electron cycle. It confirms that in diatoms as well as in green organisms, the cycle is going through the Q_B binding niche (Falkowski and Kolber, 1986).

5 Summary

Four photosynthetic mutants of the diatom *Phaeodactylum tricornutum* were characterized. These are the first photosynthetic mutants in a diatom. All mutations are found within or near the Q_B binding pocket in the D1 protein of Photosystem II (PS II). Amino acid exchanges occurred at position 219 from Valine to Isoleucine (VI-219), at position 255 from Phenylalanine to Isoleucine (FI-255), at position 264 from Serine to Alanine (SA-264) and at position 275 from Leucine to Tryptophan (LW-275). The electron transport rate, the resistance to DCMU, the architecture of the photosystems and photoprotective mechanisms were studied. VI-219 showed no impairment in electron transport and low resistance to DCMU. The amount of PS II and the antenna size of the PS II reaction centres differed only little from the WT. This was also found for the photoprotective mechanisms NPQ and the PS II cycle. FI-255 was impaired in electron transport by a factor of 1.27 and showed resistance to DCMU (300 fold). The amount of PS II was increased and the antenna size per PS II decreased. Values for NPQ were lower compared to WT and a maximum of about 6 electrons were found to cycle around PS II. SA-264 was impaired by the same factor as FI-255 but showed very high resistance to DCMU (3000 fold). As in FI-255 an increase in the amount of PS II and a decrease in the antenna size per PS II was observed. NPQ was very low as well as the electron cycling around PS II. LW-275 showed the highest impairment in electron transport and was resistant to DCMU by a factor of 500. As in the mutants FI-255 and SA-264, PS II was increased and the antenna size decreased. In addition the stochiometry of PS I/PS II was increased. The values for NPQ were the lowest in LW-275 and cycle around PS II was very high with a maximum of 7 electrons per PS II.

By characterizing the photosynthetic properties of the mutants, the importance of the four amino acids that were exchanged can be evaluated. The electron transport but also processes involved in photosynthesis such as photoprotection and light harvesting were affected. Despite the amino acids that are located close or within the Q_B binding pocket (position 255 and 264), the amino acid at position 275 seems to have a crucial role even in the functionality of the PS II.

6 References:

Arntzen CJ and Pakrasi HB (1986) Photosystem II reaction center: Polypeptide subunits and functional cofactors. In Photosynthesis III – Encyclopedia of Plant Physiology, New Series, Vol. **19**, LA Staehelin and CJ Arntzen, eds (Berlin: Springer Verlag) 457 – 467.

Barbato R, Friso G, Ponticos M and Barber J (1995) characterization of the Light-induced Cross-linking of the α-Subunit of Cytochrome b_{559} and the D1 Protein in Isolated Photosystem II Reaction Centers. *J. Biol. Chem*. **270**: 24032 – 24037.

Barber J and Andersson B (1992) Too much of a good thing: light can be bad for photosynthesis. *Trends Biochem. Sci*. **17**: 61 – 66.

Barber J and De Las Rivas J (1993) A functional model for the role of cytochrome b-559 in the protection against donor and acceptor side photoinhibition. *Proc. Natl. Acad. Sci. USA* **90**: 10942 – 10946.

Bradford MM (1976) A rapid and sensitive method for the quantitation of microgram quatities of protein utilizing the protein-dye binding. *Anal. Biochem*. **72**: 248 – 254.

Britt D (1996) Oxygen evolution. In: Ort DR, Yocum CF, eds. *Oxygenic photosynthesis: The light reactions*. Dordrecht: Kluwer Academic Publishers.

Chiesa D, Friso G, Deák Z, Vass I, Barber J and Nixon PJ (1997) Reduced turnover of the D1 polypeptide and photoactivation of electron transfer in novel herbicide resistant mutants on Synechocystis sp. PCC 6803. *Eur. J. Biochem*. **248**: 731 – 740.

Clark LC (1956) Monitor and control of blood and tissue oxygen tension. *Transactions of the American Society for Artificial Internal Organs* **2**: 41.

Delieu TD and Walker DA (1981) Polarographic measurement of photosynthetic O_2 evolution by leaf discs. *New Phytologist* **89**: 165 – 175.

Delwiche CF and Palmer JD (1997) The origin of plastids and their spread via secondary symbiosis. In: Bhattacharya D, eds. *Origins of algae and their plastids*. Springer Verlag, New York/Vienna.

Demmig-Adams B and Adams WW (1996) The role of xanthophyll cycle carotenoids in the protection of photosynthesis. *Trends Plant Sci*. **1**: 21 – 26

Diner BA and Babcock GT (1996) Structure, dynamics and energy conversion efficiency in photosystem II. In: Ort DR, Yocum CF, eds. *Oxygenic photosynthesis: The light reactions*. Dordrecht: Kluwer Academic Publishers.

Edelman M, Mattoo AK and Marder JB (1984) Three hats of the rapidly metabolised 32 kD protein of thylakoids. In: Ellis RJ ed. *Chloroplast biogenesis*. Cambridge University Press, Cambridge.

Erickson JM, Pfister K, Rahire M, Togasaki RK, Mets L and Rochaix JD (1989) Molecular and biophysical analysis of herbicide-resistant mutants of Chlamydomonas reinhardtii: Structure-function relationship of the photosystem II D1 polypeptide. *Plant Cell* **1**: 361 – 371.

Falciatore A and Bowler C (2002) Revealing the molecular secrets of marine diatoms. *Annu. Rev. Plant Biol*. 53: 109 – 130.

Falkowski PG and Kolber Z (1986) Evidence for cyclic electron flow around Photosystem II electron flow. *Plant Physiol*. **81**: 310 – 312.

Falkowski PG and Raven JA (1997) *Aquatic Photosynthesis*. Blackwell Science, Malden USA.

Falkowski PG, Barber RT and Smetacek V (1998) Biogeochemical controls and feedbacks on ocean primary production. Science 281: 200 – 206.

Gilmore AM and Yamamoto HY (1991) Zeaxanthin formation and energy-dependent fluorescence quenching in pea chloroplasts under artificially mediated linear and cyclic electron transport. *Plant Physiol*. **96**: 635 – 643.

Gilmore AM (1997) Mechanistic aspects of xanthophyll cycle-dependent photoprotection in higher plant chloroplasts and leaves. *Plant Physiol*. **99**: 197 – 209.

Guillard RRR and Ryther JH (1962) Studies of marine planktonic diatoms: 1. *C. nana* (Hustedt) and *D. confervacea* (Cleve). *Gran. Can. J. Microbiol.* **8**: 229 – 238.

Hager A and Stransky H (1970) the carotenoid pattern and the occurrence of the light-induced xanthophyll cycle in various classes of algae. V. A few members of Cryptophyceae. *Arch Mikrobiol*. **73**: 77 – 89.

Hanahan K (1983) Studies on transformation of *Escherichia coli* with plasmids. *J. Mol. Biol.* **166**: 557 – 580.

Jakob T and Wilhelm C (2001) Unusual pH-dependence of diadinoxanthin de-epoxidase activation causes chlororespiratory induced accumulation of diatoxanthin in the diatom *Phaeodactylum tricornutum*. *J. Plant Physio*l. **158**: 383 – 390.

Jeffrey SW and Humphrey GF (1975) New spectrophotometric equation for determining chlorophyll *a*, *b*, *c*1 and *c*2. *Biochem. Physiol. Pflanz.* **167**: 194 – 204.

Joliot P and Joliot A (1968) A polarographic method for detection of oxygen production and reduction of hill reagent by isolated chloroplasts. *Biochim. Biophys. Acta* **153**: 625 – 634.

Joliot P, Barbieri G and Chabaud R (1969) Un nouveau modèle photochimiques du système II. *Photochem. Photobiol.* **10**: 309 – 329.

Kafatos FC, Jones CW and Efstratiadis A (1979) Determination of nucleic acid sequence homologies and relative concentrations by dot hybridization procedure. *Nucl. Acids Res.* **24**: 1541 – 1552.

Kautsky H, Appel W and Amann H (1960) Chlorophyllfluoreszenz und Kohlensäureassimilation. *Biochemische Zeitschrift* **322**: 277 – 292.

Kok B, Forbush B and McGloin M (1970) Cooperation of charges in photosynthetic O_2 evolution – I. A linear four step mechanism. *Photochem. Photobiol.* **11**: 457 – 475.

Kooistra WH, De Stefano M, Mann DG and Medlin LK (2003) The phylogeny of the diatoms. *Prog. Mol. Subcell Biol*. **33**: 59 – 97.

Krause GH and Weis E (1991) Chlorophyll fluoresccence and photosynthesis: the basics. *Ann. Rev. Plant Physiol. Plant Mol. Biol.* **42**: 313 – 349.

Kroth P and Strotmann H (1999) Diatom plastids: Secondary endocytobiosis, plastid genome and protein import. *Physiol. Plant*. **107**: 136 – 141.

Laemmli UK (1970) Cleavage of structural proteins during the assembly of the head of bacteriophage T4. *Nature* **227**: 680 – 685.

Lavaud J (2002a) Stratégies d'adaptation des diatomées phytoplanctoniques aux variations de l'intensité lumineuse rencontrées dans leur environnement naturel. Thèse de doctorat de l'université Paris VI, University of Paris.

Lavaud J, van Gorkom HJ and Etienne A-L (2002b) Photosystem II electron transfer cycle and chlororespiration in planktonic diatoms. *Photosynth. Res.* **74**: 51 – 59.

Lavaud J, Rousseau B, van Gorkom HJ and Etienne A-L (2002c) Influence of the diadinoxanthin pool size on photoprotection in the marine planktonic diatom *Phaeodactylum tricornutum*. *Plant Physiol.* **129**: 1398 – 1406.

Lavaud J, Rousseau B and Etienne A-L (2002d) In diatoms, a transthylakoid proton gradient alone is not sufficient for non-photochemical fluorescence quenching. *FEBS Lett.* **523**: 163 – 166.

Lavaud J, Rousseau B and Etienne A-L (2003) Enrichment of the light-harvesting complex in diadinoxanthin and implications for the non-photochemical fluorescence quenching in diatoms. *Biochemistry* **42**: 5802 – 5808.

Lavaud J, Rousseau B and Etienne A-L (2004) General features of photoprotection by energy dissipation in planktonic diatoms (*Bacillariophyceae*). *J. Phycol.* **40**: 130 – 137.

Lemasson C and Etienne A-L (1975) Photo-inactivation of system II centers by carbonyl cyanide *m*-chlorophenylhydrazone in *Chlorella pyrenoidosa*. *Biochim. Biophys. Acta* **408**: 135 – 142.

Martinson TA, Ikeuchi M and Plumley FG (1998) Oxygen-evolving diatom thylakoid membranes. *Biochim. Biophys. Acta* **1409**: 72 – 86.

Maxwell K and Johnson GN (2000) Chlorophyll fluorescence – a practical guide. *Journal of Experimental Botany* **51**: 659 – 668.

Mülhardt C (2003) *Der Experimentator: Molekularbiologie/Genomics* (4. Auflage). Elsevier GmbH, Spektrum Akademischer Verlag, Heidelberg.

Müller P, Li XP and Niyogi KK (2001) Non-photochemical quenching. A response to excess light energy. *Plant Physiol*. **125**: 1558 – 1566.

Nebdal L, Samson G and Whitmarsh J (1992) Redox state of a one electron component controls the rate of photoinhibition of Photosystem II. *Proc. Natl. Acad. Sci. USA* **89**: 7929 – 7933.

Niyogi KK (2000) Safety valves for photosynthesis. *Curr. Opin. Plant Biol*. 6: 455 – 460.

Ohad N and Hirschberg J (1990) A similar structure of the herbicide binding site in the photosystem II of plants and cyanobacteria is demonstrated by site specific mutagenesis of psbA gene. *Photosynth. Res*. **23**: 73 – 79.

Owens TG (1986) Light-harvesting function in the diatom Phaeodactylum tricornutum. *Plant Physiol*. **80**: 739 – 746.

Parésys G, Rigart C, Rousseau B, Wong AWM, Fan F, Barbier JP and Lavaud J (2005) Quantitative and qualitative evaluation of phytoplankton communities by trichromatic chlorophyll fluorescence excitation with special focus on cyanobacteria. *Water research* **39**: 911 – 921.

Pfannschmidt T, Schütze K, Fey V, Sherameti I and Oelmüller R (2003) Chloroplast redox control of nuclear gene expression-a new class of plastid signals in interorganellar communication. *Antioxid. Redox Signal*. **1**: 95 – 101.

Prasil O, Zbigniew K, Berry JA and Falkowski PG (1996) Cyclic electron flow around Photosystem II *in vivo*. *Photosynth. Res.* **48**: 395 – 410.

Quick WP and Horton P (1984) Studies on the induction of chlorophyll fluorescence in barley protoplasts. I. Factors affecting the observation of oscillations in the yield of chlorophyll fluorescence and the rate of oxygen evolution. *Proceedings of the Royal Society of London B* **220**: 361 – 370.

Ritz M, Neverov KV and Etienne A-L (1999) ΔpH-dependent fluorescence quenching and its photoprotective role in the unicellular red alga *Rhodella violacea*. *Photosynthetica* **37**: 267 – 280.

Rutherford AW, Crofts AR and Inoue Y (1982) Thermoluminescence as a probe of photosystem II photochemistry: The origin of the flash-induced glow peaks. *Biochim. Biophys. Acta* **682**: 457 – 465.

Rutherford AW (1989) Photosystem II, the water-splitting enzyme. *Trends Biochem. Sci.* **14**: 227 – 232.

Saiki RK *et al*. (1985) Enzymatic amplification of beta-globin genomic sequences and restriction site analysis for diagnosis of sickle cell anaemia. *Science* **230**: 1350 – 1354.

Sambrook J, Fritsch EF and Maniatis T (1989) Molecular Cloning: A Laboratory Manual. Cold Spring Harbor Laboratory Press, New York.

Southern EM (1975) Detection of specific sequences among DNA fragments separated by gel electrophoresis. *J. Mol. Biol.* **98**: 503 – 517.

Ting CS and Owens TG (1993) Photochemical and Nonphotochemical Fluorescence Quenching Processes in the Diatom Phaeodactylum tricornutum. *Plant Phys.* **101**: 1323 – 1330.

Tischer W and Strotmann H (1977) Relationship between inhibitor binding by chloroplasts and inhibition of photosynthetic electron transport. *Biochim. Biophys. Acta* **460**: 113 – 125.

Trebst A (1987) The three-dimensional structure of the herbicide binding niche of the reaction center polypeptides of photosystem II. *Z. Naturforsch.* **42C**: 742 – 750.

Van den Hoek C, Mann DG and Johns HM (1997) *Algae. An introduction to Phycology*. Cambridge, UK: Cambridge Univ. Press.

Vermaas WFJ, Arntzen CJ, Gu LQ and Yu CA (1983) Interactions of herbicides and azidoquinones at a photosystem II binding site in the thylakoid membrane. *Biochim. Biophys. Acta* **723**: 266 – 275.

Vermaas V, Imre V, Eggers B and Styring S (1994) Mutations of a putative ligand to the non-heme iron in Photosystem II: implications for Q_A reactivity, electron transfer and herbicide binding. *Biochim. Biophys. Acta* **1184**: 263 – 272.

Whatley JM, John P and Whatley FR (1979) From extracellular to intracellular: the establishment of mitochondria and chloroplasts. *Proc. R. Soc. London B* **204**: 164 – 187.

Whitmarsh J and Pakrasi HB (1996) Form and function of cytochrome b-559. In: Ort DR, Yocum CF, eds. *Oxygenic photosynthesis: The light reactions*. Dordrecht: Kluwer Academic Publishers.

Xiong J, Subramaniam S and Govindjee (1996) Modeling o the D1/D2 proteins and cofactors of the photosystem II reaction center: Implications for herbicide and bicarbonate binding. *Protein Science* **5**: 2054 – 2073.

Zurzolo C and Bowler C (2001) Exploring bioinorganic pattern formation in diatoms A story of polarized trafficking. *Plant Physiol*. 127: 1339 – 1345.

7 Dank

Ich danke allen, die zur Entstehung dieser Arbeit beigetragen haben, ganz besonders:

Prof. Dr. Peter Kroth für die Bereitstellung des Themas und Übernahme des Erstgutachtens,

Prof. Dr. Iwona Adamska für die Übernahme des Zweitgutachtens,

Johann Lavaud und Arne Materna für die unglaublich gute Betreuung, das fortwährende Interesse an meiner Arbeit und die stets lustigen Laboralltage,

allen anderen Mitgliedern der Arbeitsgruppe Kroth für das Interesse und die gute Arbeitsatmosphäre,

Verena Reiser für die Unterstützung bei den Western Blots und die großzügige Bereitstellung von Antikörpern,

und meinen Eltern für die finanzielle Unterstützung, ohne die mir dieses Studium nie möglich gewesen wäre.

8 Erklärung

Ich versichere hiermit, dass ich die vorliegende Arbeit mit dem Thema: **Investigations of Photosystem-II-Mutants in the diatom *Phaeodactylum tricornutum*** selbstständig verfasst und keine anderen Hilfsmittel als die angegebenen benutzt habe. Die Stellen, die anderen Werken dem Wortlaut oder dem Sinne nach entnommen sind, habe ich in jedem einzelnen Falle durch Angaben der Quelle, auch der benutzten Sekundärliteratur, als Entlehnung kenntlich gemacht.

Konstanz, 06. Oktober. 2005 _____

Unterschrift